Thermoelectrics for medical applications: Progress, Challenges, and Perspectives

Boxuan Hu,[a,#] *Xiao-Lei Shi,* [b,#] *Jin Zou,*[c,d] *and Zhi-Gang Chen*[b,*]

[a] School of Chemistry and Molecular Biosciences, The University of Queensland, Brisbane, Queensland, 4072, Australia.

[b] School of Chemistry and Physics, Queensland University of Technology, Brisbane, Queensland 4000, Australia.

[c] School of Mechanical and Ming Engineering, The University of Queensland, Brisbane, Queensland, 4072, Australia.

[d] Centre for Microscopy and Microanalysis, The University of Queensland, Brisbane, Queensland 4072, Australia.

[#] These two authors contribute equally.

E-mail: zhigang.chen@qut.edu.au (ZGC)

Abstract

Thermoelectrics, enabling the direct conversion between heat and electrical energy, exhibit great potentials for employing to localized power generation and refrigeration. Their unique characteristics, such as tunable dimension, noiselessness, stability, and portability, make thermoelectrics suitable for medication-related applications. Thermoelectric applications in medicine have received increasing attention in recent years, but the research is extensive and therefore a review is needed for a systematic summary. Here, we report a timely and comprehensive review on the field of thermoelectric-assisted related materials and their medical devices, including thermoelectric power generators and thermoelectric coolers. Different medication-related thermoelectric devices are illustrated in detail, and their underlying mechanisms are discussed. In the end, we point out the challenges and future directions on medication-related thermoelectrics. This review can act as a useful tool for guiding the design of thermoelectrics with various medical applications.

Keywords: thermoelectric, materials, generators, coolers, medication.

Content

1 Introduction

Conventional fossil fuel-based energy technologies trigger severe environmental issues, such as greenhouse emissions and water pollution [1]. To solve these issues, thermoelectrics, acting as a powerful technique to assist the reduction of power consumption, have attracted great attention in the last decades [1, 2]. Compared to other sustainable power generation techniques [3], thermoelectrics possesses many unique advantages, such as no moving parts, noise-free, long service life, zero-emission, and precise temperature control [4]. Therefore, thermoelectric materials and devices have been used in the fields of solid-state cooling, heating, and power generation. In terms of heating and cooling, thermoelectric devices (TEDs) can act as thermoelectric coolers (TECs), which can reduce the temperature on one side and increase the temperature on the other side by applying direct current (DC) [5]. By changing the direction of the current, TECs can be switched between cooling and heating modes [6]. At the same time TECs do not use Freon compared to conventional compressor cooling, these factors give TECs a huge advantage over conventional compressors [7]. In terms of the power-generation function, TEDs can act as thermoelectric generators (TEGs), exhibiting unique advantages including flexibility, reliability, and adaptability that traditional power-generation techniques do not have [8]. The direct solid-state conversion from temperature difference (ΔT) to electricity enables them to be very suitable for space exploration and biomedicine sensors [9, 10]. Although thermoelectric technology has existed commercially since the 1950s [11], extensive research on thermoelectric medical applications begin until the 1990s and their commercialization on a large scale was until 2010 when Amerigon signed a 3-year marketing deal with Mattress Firm, Inc. for a thermoelectric heated/cooled mattress [11, 12].

Recently, TEDs have been extended to apply for wide medication [13-18], as summarized in **Figure 1**. For example, cryotherapy has been used in medication for thousands of years [19]. Whether it is a sprain, strain [20], eye disease [13], cancer [16], or brain hypoxia after a car accident [14, 15], cryotherapy can be used for instant treatment. Traditional cryotherapy often uses ice packs [20].

However, ice packs show many disadvantages such as being heavy, fitting badly with human skin, complex preparation requirements, non-lasting cooling performance, and being out of temperature control. As well, conventional cryotherapy may lead to frostbite, such as decreased decomposition of oxygen haemoglobin, increased blood viscosity, increased red blood cell hardness, and development of a hypoxic state and hinder the flow [21]. TECs, that integrate refrigeration and heating and that can quickly respond and cool, can avoid frostbite for portable use in ambulances or long-term cryotherapy of injured parts of the body [22]. Moreover, the stability and silent operation characteristics of TECs are also promising for other human body cooling, as mentioned in **Figure 1** [13, 14, 17, 18].

In addition to the cryotherapy treatment, patients have an increasing demand for biomedical sensors for health monitoring [10]. Generally, biomedical sensors require less energy than the 190 μW of output power currently generated by TEGs [23, 24]. Therefore, TEGs can support the operation of biomedical sensors and in turn increase the portability of biomedical sensors. Implantable medical devices (IMDs), which can assist or replace part of the functions of specific human tissues or organs, have a long history in clinical medicine [25]. However, both the previous nuclear batteries and the current lithium batteries have shortcomings such as toxicity and short lifetime [26]. Strong-stability, high-safety, and small-sized TEGs can meet the needs of IMD [10]. Therefore, considerable research has been devoted to the development of implantable TEGs and wearable TEGs (**Figure 1**) [10, 27, 28].

There are growing interests in medical thermoelectrics. Therefore, a timely and comprehensive review of the related research is highly needed. Here, we highlight the progress on the fundamentals, materials, and devices of thermoelectrics that target medical applications, including both TEGs and TECs. The current and potential applications of TEDs based on various scenarios are summarized. In the end, we point out the challenges and outlooks on the future development of medication-related thermoelectrics. This review will be a useful tool to guide the design of medication-related thermoelectrics.

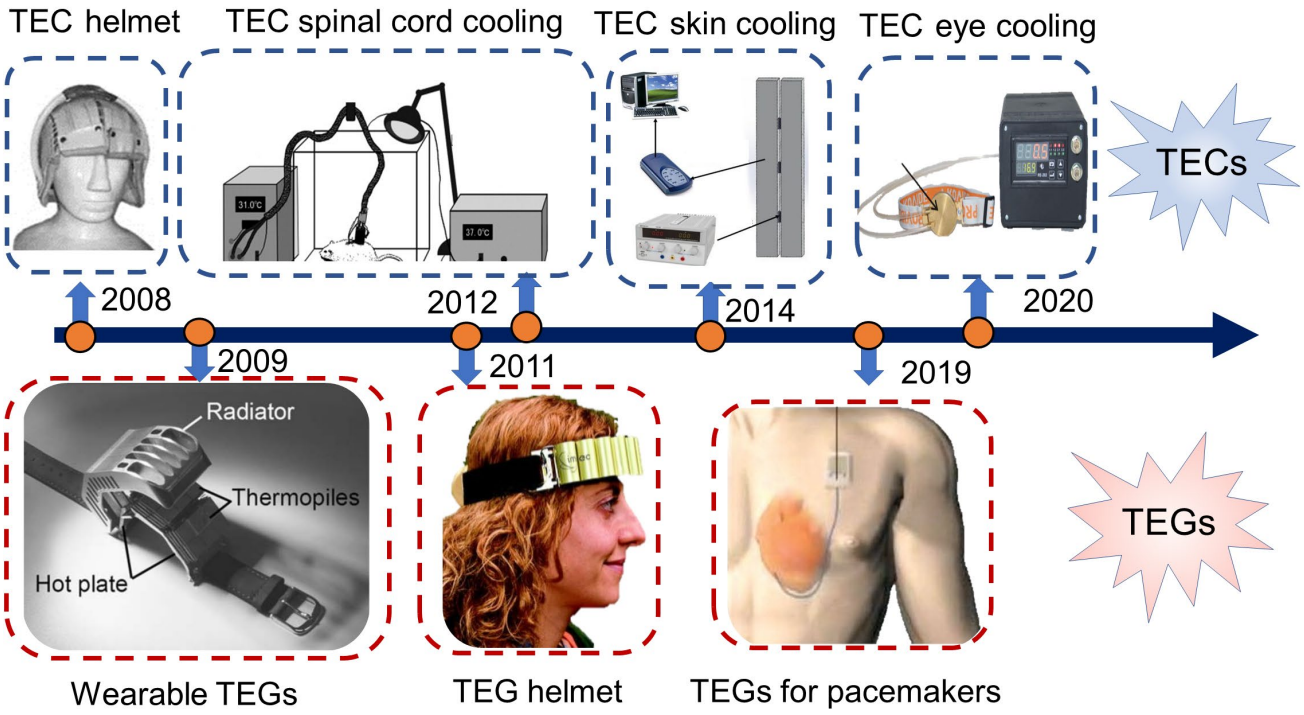

Figure 1 Current key research for medical applications of thermoelectric power generators (TEGs) and thermoelectric coolers (TECs). Portable TEC helmet, reproduced with permission [14]. Copyright 2008, Taylor & Francis Group. TEC spinal cord cooling, reproduced with permission [17]. Copyright 2012, Elsevier. TEC skin cooling, Reproduced with permission [18]. Copyright 2014, Elsevier. TEC eyes cooler, reproduced under a Creative Commons Attribution-ShareAlike 4.0 International (CC BY-SA 4.0) license [13]. Copyright 2020, OJS/PKP. Wearable TEGs, reproduced with permission [27]. Copyright 2009, Springer. TEG helmet, reproduced with permission [28]. Copyright 2011, Springer. TEGs for pacemakers, reproduced under a Creative Commons Attribution-ShareAlike 4.0 International (CC BY-SA 4.0) license [10]. Copyright 2019, MDPI.

2 Principle

2.1 Basic parameters

Thermoelectric effects used in the medication field include the Peltier effect, the Seebeck effect, and the Thomson effect [29]. Generally, medical applications mostly involve the Peltier effect and the Seebeck effect. The Seebeck effect refers to the ability to generate electricity by converting the ΔT

between the two sides of the thermoelectric material, while the Peltier effect is the transfer of heat from the cold side of the thermoelectric material to the hot side, driven by an imposed electricity [4]. The Thomson effect is that the temperature difference between any two points of a current-carrying conductor causes heat to be absorbed or released, depending on the direction of the current and the material [30]. For medical TEDs, the Thomson effect can reduce the amount of energy required. The dimensionless figure of merit, *ZT*, is widely used to evaluate thermoelectric materials [31], expressed as:

$$ZT = \frac{S^2 \sigma T}{\kappa} \tag{1}$$

where *S* is the Seebeck coefficient, *T* is the absolute temperature, σ is the electrical conductivity, and κ is the thermal conductivity. In addition to *ZT*, Carnot efficiency ϕc is an important performance parameter [4], expressed as:

$$\phi c = \frac{T_{\mathrm{H}} - T_{\mathrm{C}}}{T_{\mathrm{H}}} \tag{2}$$

where T_{H} is the temperature on the hot side, T_{C} is the temperature on the cold side. TEDs depend on the ΔT between the two sides as well as their own performance. The maximum thermoelectric conversion efficiency (η_{max}) can be obtained by combining the Carnot efficiency and *ZT* [32], expressed as:

$$\eta_{max} = \left(\frac{T_{\mathrm{H}} - T_{\mathrm{C}}}{T_{\mathrm{H}}}\right) \cdot \left(\frac{\sqrt{1+ZT} - 1}{\sqrt{1+ZT} + \frac{T_{\mathrm{C}}}{T_{\mathrm{H}}}}\right) \tag{3}$$

For organic materials, the value of *ZT* cannot be accurately calculated and power factor ($S^2\sigma$) is required to effectively characterize the properties [32]. The most direct way to improve the thermoelectric properties of both organic and inorganic materials is to increase *S* and σ [33]. For inorganic thermoelectric materials, band engineering is widely used to tune the carrier concentration for increasing σ or *S* [33, 34]. Meanwhile, rational resonant doping can effectively enhance *S* [3], while energy filtering enables selectively blocking lower energy carriers and enhancing the *S* with only a

small loss of σ [35]. The current device efficiencies of medical TEDs are mainly determined by their internal thermoelectric module, which are expected to be further enhanced by improving the thermoelectric performance of thermoelectric materials.

2.2 Thermoelectric materials

The core body temperature of the human body is between 36.5 and 38.5°C [36]. This means that the ΔT between the human body and medical TECs or TEGs operating at room temperature of 300 K is only ~10 K. Together with volume constraints, medical devices should require high-performance thermoelectric materials with high near-room-temperature thermoelectric performance [32]. Generally, thermoelectric materials can be divided into one-dimensional (1D), two-dimensional (2D), and three-dimensional (3D) materials. 3D materials are predominantly bulk semiconductor materials, as semiconductors have higher thermoelectric properties than metallic materials [31]. Most conventional thermoelectric bulk materials are inorganic compounds, of which Bi_2Te_3 was the first thermoelectric material to be developed [31, 32] and still is the best thermoelectric material at room temperature [1, 31]. Hence, all TEDs used for medical applications almost utilize bulk Bi_2Te_3-based materials. Meanwhile, various methods have been developed to increase *ZT* values of Bi_2Te_3-based materials, such as nano-structuring [37-39], carrier concentration optimization [40, 41], and band engineering [42] **Figure 2a** summarize a few art-of-state bulk materials, including Bi_2Te_3 [43, 44], Mg_3Sb_2 [45], SnSe [46], SnTe [47], GeTe [48], PbTe [49], Cu_2Se [50], Zintls [51], $SrTiO_3$ [52], BiCuSeO [51], Half-Heuslers [53], and Skutterudites [54]. In addition to conventional Bi_2Te_3-based thermoelectric materials, some newly developed thermoelectric materials have shown promising near-room-temperature *ZT* values. For example, as a typical transition metal selenium compound, Cu_2Se has a high *ZT* of >2.0 at high temperatures, and can be used to prepare inorganic thermoelectric films by the

magnetron sputtering or thermal evaporation [50, 55-57]. A promising room-temperature *ZT* of 0.35 has been observed in Cu_2Se, prepared by an efficient layer-by-layer combination reaction method, and such a *ZT* can be maintained after 800 bending cycles [55]. Therefore, Cu_2Se shows potential to be used in medical applications. Till now, bulk thermoelectric materials with high *ZT*s at lower temperatures are suitable for designing TEDs that target current medication applications.

2D thermoelectric materials are mainly thermoelectric thin films. Although conventional bulk materials show high *ZT* values at room temperature, these materials are difficult to be used in flexible TEDs due to their rigidity and brittleness [58, 59]. 2D inorganic thermoelectric materials have certain flexibility and acceptable thermoelectric properties, showing high potential for flexible TEDs [58]. In the last few years, inorganic Ag_2Se and Bi_2Te_3 based films [60-64] show high flexibility, indicating the potential of inorganic flexible TEDs [65, 66]. In terms of organic thermoelectric materials, they are ideal for flexible TEDs due to their superior flexibility and ability to maintain performance at low temperatures [58]. Many organic thin-film materials, including poly(3,4-ethylenedioxythiophene) polystyrene sulfonate (PEDOT:PSS) [67], have already been used in the design of flexible TEDs [68-71]. As a promising flexible thermoelectric material, organic PEDOT:PSS has received great attention because of its intrinsic low κ [72]. Its thermoelectric performance can be improved by different strategies, including doping [73], secondary doping [74], and pre- or post-treatment [71]. A few doping methods, such as chemical doping [75], electrochemical doping [76], and protonic acid doping [77], have been developed to tune the σ of PEDOT:PSS. With increasing the doping concentration, the carrier concentration of PEDOT: PSS increases, which improves the σ but decreases the *S* of PEDOT:PSS. Potential-step chronocoulometry (PSC) can be used to confirm the correlation between doping levels, as well as to confirm the situation [78, 79]. As well, secondary doping is an important

way to improve the thermoelectric properties of PEDOT:PSS, which is able to combine with doping engineering to simultaneously increase σ and S [80]. At the same time, oxidation also affects the performance of the doped PEDOT:PSS [81, 82]. Furthermore, post-treatment can improve the σ by changing the structures or enhance the S by adjusting the excessive carrier concentration in PEDOT:PSS [71], which effectively decouple the σ and S. It was reported that triple post-treated PEDOT:PSS has a high $S^2\sigma$ of 141 μW m^{-1} K^{-2} at room temperature [71]. Besides, PEDOT:PSS can be combined with other substances to form new composites with further improved performance. For example, PEDOT:PSS/single-walled carbon nanotube film (PEDOT:PSS/SWCNT) composite, prepared using ionic liquid additives, shows a $S^2\sigma$ of 301.35 μW m^{-1} K^{-2} and a higher elongation [83]. Besides, high-performance PEDOT:PSS/SWCNT can be prepared by simply mixing aqueous dispersions of SWCNT and PEDOT:PSS in different weight ratios and soaking them in DMSO for 2 minutes at room temperature. The PSC can measure the carrier density in each doping state, and analyse the carrier mobility and σ [84, 85]. By integrating with polydimethylsiloxane (PDMS), these PEDOT:PSS-based composites show better flexibility [86]. The doping of sulfonated polysiloxane (PSiPS) into PEDOT can improve the self-supporting properties and flexibility while maintaining similar thermoelectric properties to PEDOT:PSS [87].

Other organic thermoelectric materials also show high thermoelectric properties. For example, poly(3-hexylthiophene) (P3HT) has a maximum $S^2\sigma$ of 325 ± 101 μW m^{-1} K^{-2} [88], and polyaniline (PANI) shows a maximum $S^2\sigma$ of 407 μW m^{-1} K^{-2} [89]. These high room-temperature $S^2\sigma$ achieved in flexible thermoelectric materials are promising for applying to medical applications [72]. Meanwhile, by combination with photovoltaic devices, TEDs show much high power densities to expand their medical applications [90]. However, both TECs and TEGs require a high level of device performance

and stability for medical applications. Currently, the performance of thin film materials, especially organic films, is still below that of bulk materials [77], making them difficult to use for medical applications.

1D thermoelectric materials, such as nanowires and fibers, have been extensively studied recently [91, 92]. For example, silicon nanowires have a *ZT* value of nearly 1 at 200 K [93], which provides the basis for their applications [91]. However, the synthesis of these materials is not mature enough, and the choice of catalyst, for example, is still not resolved [94]. Therefore, 1D materials are challengeable for being used in the medical field in a short term.

2.3 Thermoelectric devices

Thermoelectric modules can be designed into different types of TEDs depending on the requirements, and can be divided into conventional modules, miniature devices, and flexible devices. On this basis, there are also two different types of devices, namely single-stage and multi-stage. Generally, compared to conventional cooling and power generation techniques, the efficiencies of current TEDs are still not competitive enough [95, 96], and in turn multi-stage devices are often used instead of single-stage devices to increase performance and portability while reducing size. A study shows that two-stage TECs require only half the current of single-stage TECs to reach the peak of the Rate of Refrigeration (ROR) and Coefficient of Performance (COP) [97]. The COP and ROR of two-stage TECs are lower than those of single-stage TECs because the number of TE elements on the cold side of two-stage TECs is less [97]. If the number of stages is further increased, the ultimate cooling or power generation capacity of the thermoelectric material can be further increased.

Thermoelectric modules are generally made up of a combination of p-type and n-type thermoelectric legs [98]. These conventional modules become double-leg modules and can be divided into π-types [99], O-types [100], and Y-types [101]. The π-type thermoelectric module is more often used for biomedical applications, and the technology is relatively mature. The π-type devices require

the rational selection of suitable n- and p-leg materials to ensure high thermoelectric performance that can be maintained over a long period, and the design of the interlayers that connect the thermoelectric legs to the electrodes can reduce the impact of external forces and thermal shocks on the device, and increase thermoelectric power and conversion efficiency [102]. These issues are generally approached using appropriate device construction, dimensioning, material selection, and interlayer design to achieve a high-performance and stable thermoelectric module [1]. Single-leg modules are often used when the performance and thermoelectric conversion efficiency of the p- leg or n-leg needs to be evaluated [103], as shown in **Figure 2b**.

With the development of integrated circuits and microelectronic systems, medical devices, such as biosensors, consume less energy and require a high power density and long-life micropower source to replace conventional batteries or alternating current/direct current (AC/DC) power sources [104]. Miniature TEDs can meet these needs by harnessing the ΔT to generate power and are especially suitable for integrating biosensors with low energy-consumptions [105], as shown in **Figure 2c** [106]. Miniature TEDs, such as implantable medical TECs, can be used to cool the target area more quickly [107]. Therefore, miniature TEDs have attracted considerable attention, despite the fact that miniature TEDs are technically complex to manufacture and have lower performance than conventional TEDs [108].

In addition to the performance, comfortability is a consideration when used for wearing, and flexible TEDs are less likely to be structurally damaged when under bending, making them the good choice for wearable devices [109], as shown in **Figure 2d**. Many wearable medical TEGs and TECs adopt a flexible design. Flexible TEDs can be divided into those made from flexible organic materials [110] and those made by printing onto a flexible substrate [109]. The former uses mainly thin-film materials such as PEDOT:PSS, which takes advantage of their inherent flexibility [111-114], while the latter uses bulk materials such as Bi_2Te_3 printed onto organic substrates such as PDMS and polyimide [115-122]. Since conventional bulk materials have higher thermoelectric performance than thin-film

materials, flexible TEDs for biomedical devices are mostly designed for the second preparation method [1, 109]. In such TEDs, high flexibility and long service life are both important. Therefore, a rational structural design of TEDs is required to improve their flexibility, stability, and comfortability.

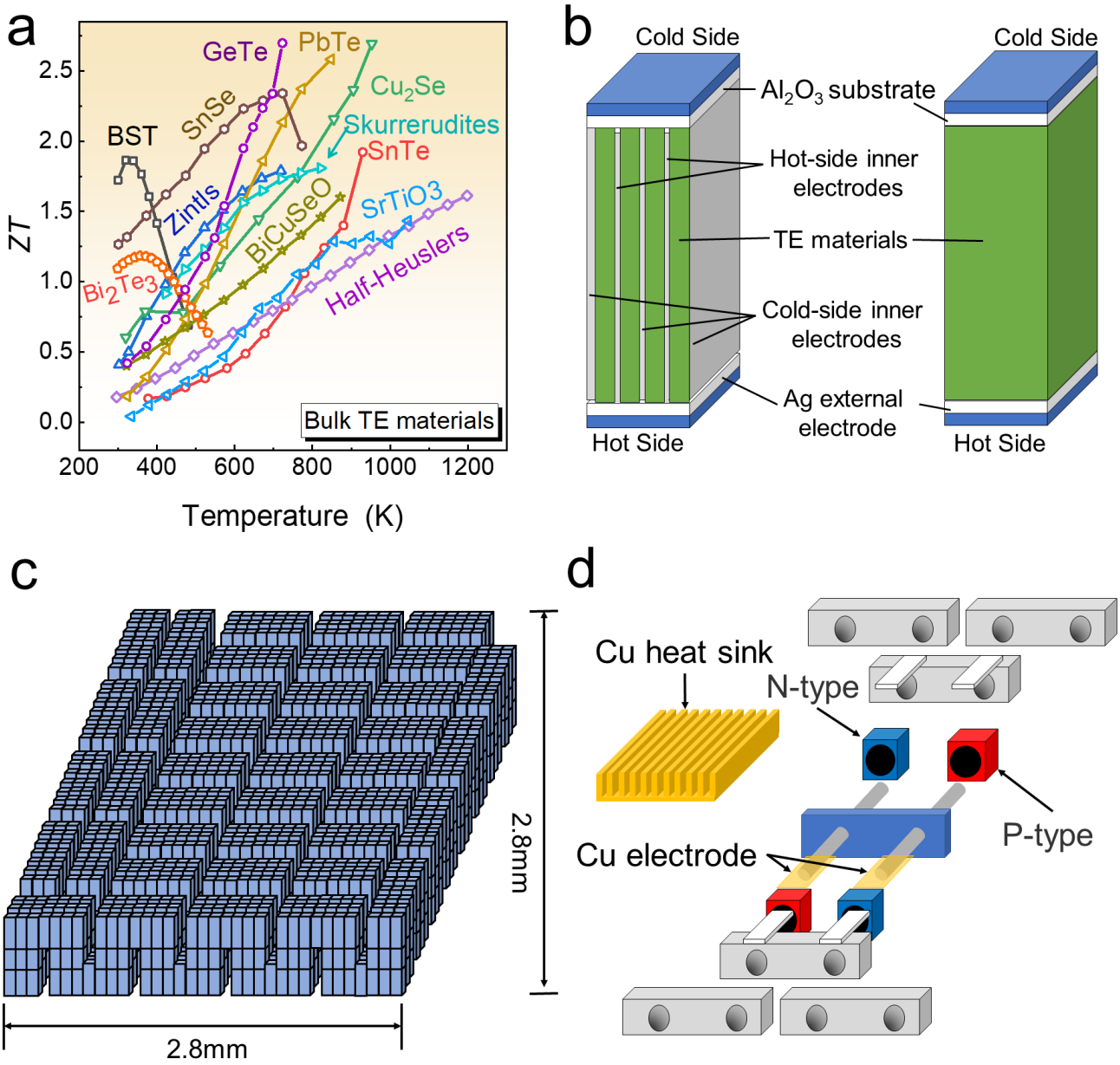

Figure 2 a) Reported state-of-the-art bulk thermoelectric materials for peak *ZT* values [43-54]. b) Two different types of single-leg modules. Reproduced with permission [103]. Copyright 2020, Royal Society of Chemistry. c) Diagram of miniature thermoelectric devices (TEDs). Reproduced with permission [106]. Copyright 2012, Elsevier. d) Diagram of flexible TEDs. Reproduced with permission [109]. Copyright 2017, Elsevier.

3 Medical applications

TECs can be used for a wide range of medical applications, such as cryosurgery, skin cooling, and the preservation of medical and biological products [123]. Currently, TECs have already been used in portable refrigerators, which allow efficient storage and transport of medical and biological products to prevent medical accidents [124-126]. As well, with the rapid development of wearable biomedicine sensors and portable therapeutic devices, the demands for TEDs with high reliability, noise-free operation, and ease of handling are huge [58, 127, 128]. **Table 1** summarises the performance of TEDs in medications reported in recent years.

Table 1 An overview of performance of thermoelectric devices in medications.

Year	Type	Application	Max ΔT (K)	Lowest Temperature (°C)	Output Voltage (mV)	Output Power (mW)	Reference
2008	Wearable TECs	Brain Cooler	34.2	−6.75	-	-	[14]
2005	Wearable TECs	Brain Cooler	34.5	−6.87	-	-	[15]
2018	Wearable TECs	Skin Cooler	-	3.00	-	-	[22]
2018	Wearable TECs	Skin Cooler	-	4.00			[129]
2014	Wearable TECs	Skin Cooler	44.7	7.59	-	-	[18]
2010	TEC Cryoprobe	Cryosurgery	117.0	-88.79	-	-	[16]
1993	TEC Cryoprobe	Cryosurgery	65.5	-51.99	-	-	[12]
2010	Implanted TECs	Suppress Epilepsy	-	16.11	-	-	[107]
2007	Implanted TEGs	Power generation for IMDs	-	-	12.77	-	[130]
2013	Implanted TEGs	Power generation for IMDs	-	-	19.07	0.03	[25]
2017	Wearable TEGs	Power generation for biomedicine sensors	-	-	11.27	-	[105]
2016	Wearable TEGs	Power generation for biomedicine	-	-	-	156.78	[24]

		sensors					

3.1 Thermoelectric coolers

Compared to conventional skin cooling methods, TECs have no physical attachment and can realize direct cooling by simply using the current for a long time and avoiding frostbite [123]. The small-size and noise-free features make TECs possible to be employed in situations where delicate devices and a quiet environment are required, such as in surgery or car accidents [58, 127, 128].

3.1.1 Brain cooler

The protection of the patient's brain is often a difficult issue in the event of a traffic accident or cardiovascular surgery. To improve the survival rate of patients with traumatic brain injury, patients should be treated as soon as possible. Nearly 20% of patients die from lack of oxygen in the brain as a result of not being able to receive treatment in the first place [14]. This is because the injured brain often requires a greater supply of oxygen and is less tolerant of hypoxia [131-134]. There is a risk of ischaemic brain injury during uncontrolled bleeding and cardiovascular surgery [14, 135]. Cranio-Cerebral Hypothermia (CCH) is commonly used to reduce the enzymatic reactions in brain cells and the rate of cellular metabolism, which reduces oxygen demand and increases patient survival [131, 133]. Traditionally, ice packs can be placed on the head or the patient's head can be placed in cold water to achieve the goal [123]. However, these methods have disadvantages such as inefficient refrigeration, stockpiling of ice water and ice, and difficulties in transport [123]. TEC helmets can operate at DC voltage in ambulances and thus accompany ambulance personnel and provide faster first aid to patients [14].

As wearable TECs, the comfortability of wearing should be considered. Flexible TEDs have been designed to be fitted with the patient's head and in turn to increase the operational life of the instrument [14]. **Figure 3a** shows the heating and cooling performance of TECs and the inset is the as-designed TEC helmet, which consists of 120 flexible thermoelectric modules connected in series to support up to a current of 40 A, paired with a portable water circulation system for water cooling [14]. Such a

TEC helmet can be optimized by using an Adaptive Neuro-Fuzzy Inference System (ANFIS) [14]. By running multiple cooling cycles under the control of ANFIS, the cooling rate of the device can be optimized. As shown in **Figure 3a**, the temperature drops to -2 °C in ~6 minutes after the cooling is switched on and then stabilizes at -1 °C. [14]. When switching to the heating mode, the temperature can reach 31°C in ~5 minutes, and stabilize at 30 °C after ~6 minutes [14]. Both modes can run steadily for more than 1 hour [14], which is sufficient for transporting the patients to the hospital. The power can be further increased if used in a hospital. **Figure 3b** shows the ΔT when the device is operating at different power levels. As the power increases, the ΔT between the hot and cold sides of the device also rises. At 13 W, a ΔT of 13 K can be produced, while at 300W, a ΔT of close to 35 K can be produced and the cold side can be reduced to -6 °C. Such a performance already meets the need of most scenarios [14].

Figure 3c shows another TEC helmet, which is connected to a pump and a water tank to enhance its cooling capacity by pumping a stream of water to cool the device [15]. Although it is still designed to perform CCH to increase patient survival rates, it is more suitable for use in open areas such as hospitals than ambulances by a large cooling system. In combination with the human brain hypothermia system, the temperature of the helmet can be controlled by the microcontroller between -5 °C and 46 °C [15]. **Figure 3d** shows the cooling effect of the TEC helmet at different currents. With the aid of water cooling, a current of 30 A enables the cold-side temperature to be below -6.87 °C for 3 minutes, meeting the CCH requirements which require an operating temperature of -5 °C [15]. When the current is reduced to 25 A, the cold-side temperature is dropped to -5.03 °C, which is exactly the required temperature. Such a TEC helmet can effectively improve patient survival [15]. However, in terms of a TEC helmet that can be installed and operated in an ambulance, a balance needs to be considered between performance and power.

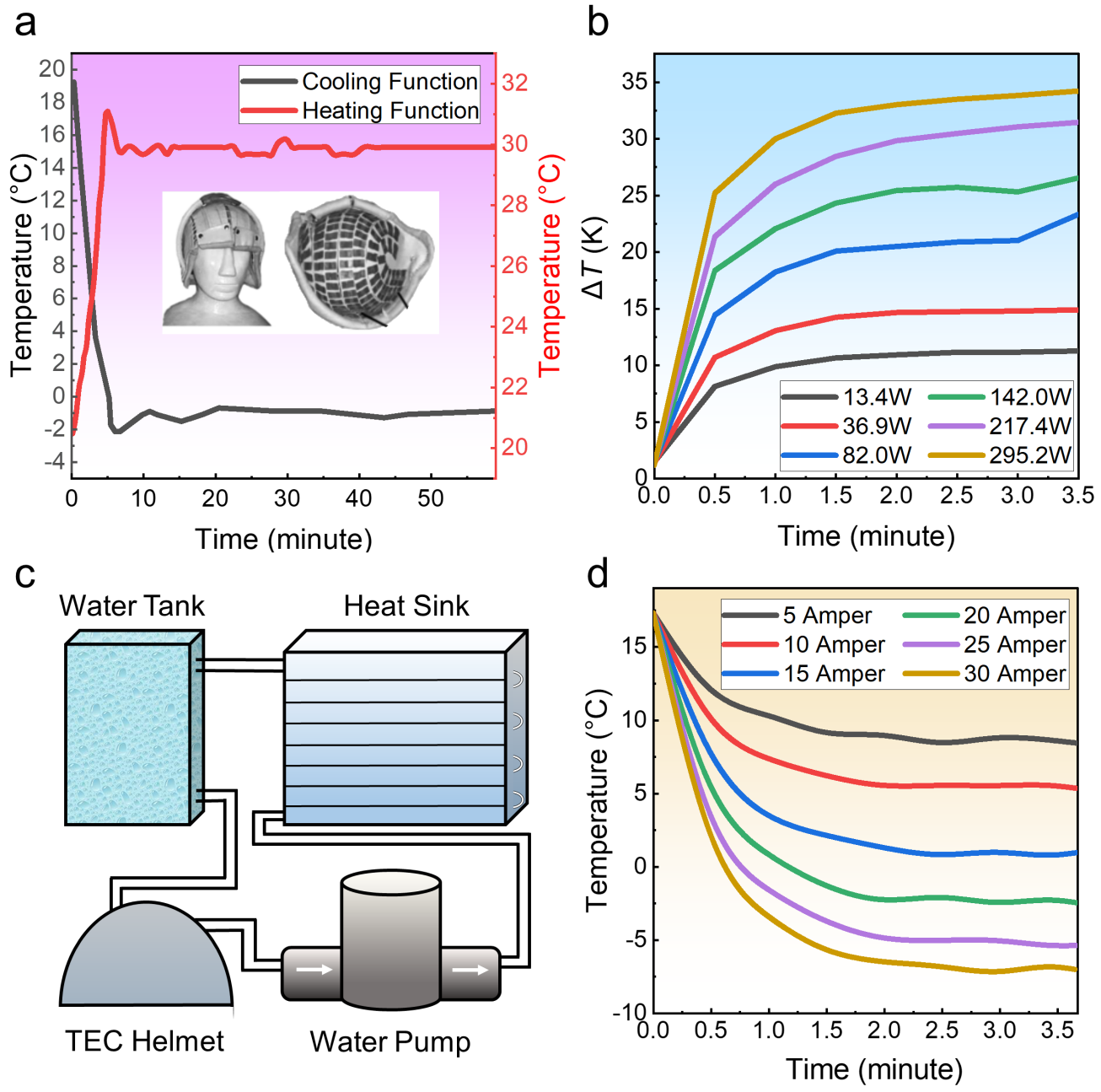

Figure 3 a) Cooling and heating effect of a thermoelectric cooler (TEC) helmet and its finished diagram. b) Temperature difference (ΔT) of a TEC helmet at different power. Reproduced with permission [14]. Copyright 2008, Taylor & Francis Group. c) Schematic diagram of a TEC helmet cooled down using a water pump. d) Variation of temperature on the cold side of a TEC helmet at different currents. Reproduced with permission [15]. Copyright 2005, Springer.

3.1.2 Suppress epilepsy

In addition to performing CCH, by applying targeted cooling directly to a fixed part of the brain, TECs can also be used to treat some brain disorders, such as epilepsy [107]. Epilepsy is a serious chronic neurological condition that affects approximately 65 million people worldwide [136]. Conventional treatment options include medication and surgery [107]. However, anti-epileptic drugs are expensive and treatment rates are not ensured [107, 137], while some types of epilepsy cannot be treated surgically [107]. Hence, it is urgent for developing a new and effective treatment for epilepsy. Nearly 60 years ago, it was found that the cryogenic treatment of the brain could suppress epileptic discharges (EDs) [138, 139], which is now possible to be realized by TECs. Miniature TECs possess great potential to suppress EDs by mounting in multiple brain gully. **Figure 4a** shows a schematic diagram of implantable TECs used for the treatment of epilepsy. Its core component is a 4mm × 4mm × 2mm TEC chip. The chip is fitted with an aluminium heat sink, and connected to the circulation system via two silicone tubes for maintaining the water temperature at 37°C. The temperature drop is monitored by adding a thermocouple under the TEC chip [107]. The EDs were induced by injecting 3 mg/l of kainic acid (KA) into the brains of experimental animals at 1 μl [107]. The hippocampal seizure was simulated by injecting KA into the left hippocampus, and electrodes were inserted into the right hippocampus to measure the ED changes in the hippocampus [107]. **Figure 4b** shows the effect on brain waves before and after the TEC was switched on. The EDs were more intense at the beginning of the measurement and after rewarming, while benefiting from the cooling of the TEC. The electroencephalogram (EEG) showed a weak signal of EDs [107]. **Figure 4c** shows the change in brain surface temperature after the device was switched on. **Figure 4d** displays the difference in EDs amplitude after the device was switched on compared to the control group. The combination of **Figure 4c** and **Figure 4d** can be determined the EDs amplitude, which was suppressed as the temperature decreased and eventually dropped to 68.1%. As the TEC was switched off and the temperature began to rise, the EDs amplitude eventually recovered to 85%, similar to 95% of the control group at the

same time. This indicates that a temperature decrease of approximately 20 °C by TECs is the optimal temperature for terminating seizures in the hippocampus. Similar experiments have demonstrated that the optimal TEC temperature for terminating seizures in the cortical surface is almost identical to that in the hippocampus [107, 140, 141].

For a medical device used to treat epilepsy, animal testing alone was not sufficient. After approval, Masami FUJII et al. conducted clinical trials [107]. During surgical treatment of patients with intractable epilepsy, the area where EDs were present was cooled using TECs instead of excisional surgery on the target area [107]. The results are shown in **Figure 4e**. When the TECs were operated, the temperature was rapidly reduced to ~18 °C. During this process, the EDs were substantially suppressed when the patient's brain was cooled to below 25°C [107]. Although clinical and animal studies have demonstrated that cooling to ~20 °C does not cause irreversible damage to the brain, it is still important to determine the minimum safe temperature for safety reasons. By comparing the control group for cortical cells after being cooled to -5 °C and 0 °C within one hour (**Figures 4f, 4g, 4h**), it can be seen that the temperature that causes irreversible damage is -5 °C, and 0 °C is safe [107]. The same results were also demonstrated by long-term experiments on rat and cat brains. Therefore, it can be concluded that when the brain is cooled to between 0 °C and 20 °C, only local synaptic activity is disrupted. This suggests that the used TECs are safe [107, 142]. The location of thermocouples can impact this type of TEC chip. A previous study showed that the built-in thermocouple can measure transient temperature changes in the brain more accurately and sensitively than the external thermocouple, which may help to accurately adjust the execution temperature of TECs [143]. However, other supporting devices such as heat dissipation and power supplies cannot be miniaturized, and if there is a breakthrough in the miniaturization of TECs, implantable TEC devices could be used to treat brain diseases.

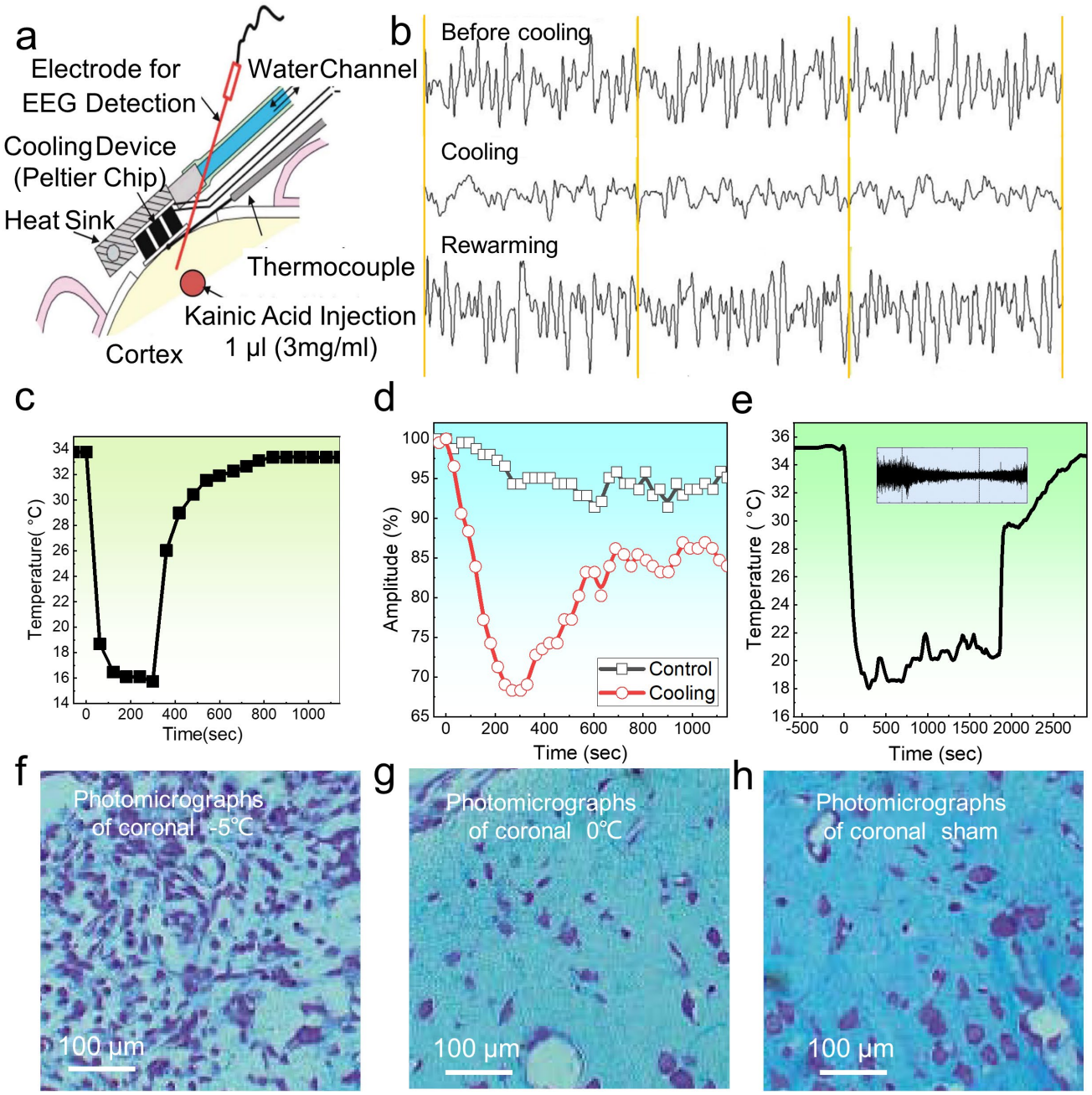

Figure 4 a) Schematic diagram of the thermoelectric cooler for the treatment of epilepsy. b) Amplitude of brain waves in different cooling states. s) Temperature of the cerebral cortex in different cooling states. d) Comparison of the amplitude of epileptic discharges (EDs) in the control and cooling groups. e) Temperature of the human brain during human experiments with EDs. f) Coronal micrographs at -5 °C. g) Coronal micrographs at 0 °C. H) Coronal micrographs at Sham control. Reproduced under a Creative Commons [Attribution-NonCommercial-NoDerivatives 4.0 International] license [107]. Copyright 2010, J-STAGE.

3.1.3 Cryosurgery

In addition to treating epilepsy, TECs can make cryoprobes perform cryosurgery. Cervical cancer is one of the most common malignancies in the world, with 7,500 people dying from it every year in Indonesia alone [16]. Using a cryoprobe instead of a scalpel for cutting can avoid post-operative infections and ugly scars, as well as reduce the patient's pain during the procedure [16]. Traditional cryoprobes are cooled with liquid nitrogen, dry ice, chlorofluorocarbons, and nitrous oxide, which are often environmentally contaminated or toxic to patients and doctors, and cost considerable money to prepare and store due to their tendency to evaporate [16]. In order to expand the utility of cryosurgery, multi-stage TECs with faster and more reliable cooling capacity can be used instead of traditional refrigerants for cutting the exact body part [16].

Figure 5a shows the structure of the TEC cryoprobe [16]. The main body of the cryoprobe is a multi-stage TECs with a cold side of 5 mm × 5 mm and a hot side of 40 mm × 40 mm. The hot side is directly in contact with the heat sink baseplate, which is connected to four copper heat pipes [16]. Fins can be added to the heat sink for auxiliary heat sinking, and the top is connected to a circulating thermostatic bath (CTB). Such a TEC cryoprobe can be controlled by a computer terminal operation [16]. In order to clarify the most appropriate stage of the TEC cryoprobes, the cooling capacity of 5 and 6 TECs was evaluated (**Figure 5b**) [16]. When the CTB is controlled at 303.15 K, 6 TECs can be cooled to 195 K, close to the dry ice temperature for cryosurgery, whereas 5 TECs can only be reduced to 211 K [16]. **Figure 5c** shows the variation of ΔT at different CTB temperatures. **Figure 5d** illustrates the cold side temperature at different CTB temperatures. As can be seen, the ΔT rises as the CTB temperature rises. The cold-side temperature is highest when the ΔT is at its maximum (**Figure 5d**), indicating that the increased ΔT comes from the warming of the hot side rather than from the performance improvement. To improve performance, the CTB temperature should be reduced [16].

The design of the heat sink can affect the cooling capacity of the TEC cryoprobe. **Figure 5e** compares the results from different cooling methods, including air cooling, air cooling with heat pipes,

air cooling with heat pipes and fins, water cooling, water cooling with heating pipes, water cooling with heating pipes and fins [16]. The design of the heat sink using water as the cooling medium and with a finless heat pipe can reach the lowest cold side temperature up to ~184 K, while the air-cooling heat sink with no additional auxiliary cooling has the worst cooling performance with ~202 K at the cold side, indicating that the heat pipe can effectively assist with cooling [16]. However, the performance of the water cooling with both heat pipes and fins is rather inferior to the water cooling without heat pipes and fins and the air cooling with heat pipes and fins [16]. This is because water has a high convection coefficient, and the use of fins in this case leads to lower performance. However, the air is a medium with a lower convection coefficient, and thus fins in the air can enhance its cooling capacity [16].

As highly efficient heat transfer TECs with long distance and low consumption, heat pipes can be used to simultaneously sink TEC cryoprobes and assist TEC cryoprobes in the accurate cooling of the body [144]. If TECs are directly used in contact with the patient for treatment, the TECs may face problems, such as inflexibility and sensitivity to thermal intensity. However, if the TECs are combined with a heat pipe, TECs can be flexibly applied to the patient [12]. **Figure 5f** displays a schematic diagram of a TEC cryoprobe combined with a heat pipe. By combining this with **Figure 5g**, it can be seen that the temperature at the tip of the cryoprobe is similar to the temperature at the cold side of the TECs [12]. With no load, the ΔT is only 1.5 °C; while with a load of 15 W, the ΔT can be 3 °C [12]. By combining with the high-performance TEC cryoprobe in the previous case, it can achieve effective and flexible cryosurgery of patients. It should be noted that the cryoprobe is not yet flexible enough, and a new contact tip can be developed to better reduce the scarring left by the patient. During surgery, blood cells, special drugs or other biological products are often required. These essential items need to be stored and transported at a certain temperature [124]. The high portability of TEDs makes them

easier to transport than large refrigeration devices that run on Freon gas or compressors. TEDs can switch between cooling and heating functions to perfectly suit this need [124]. With the outbreak of COVID-19, the demand for vaccines is increasing. These vaccines generally need to be transported at lower temperatures (2-8 °C for AstraZeneca) [145]. At the same time, in order to ensure the immunogenicity of the vaccines, it is necessary to keep the vaccines in the cold chain at the right temperature with monitors for precise temperature control. This is because the vaccines can only be used at critical points in time after removal from the cold chain. Compared to a large freezer truck, thermoelectric storage devices offer excellent portability, making it easier to transport the right amount of vaccine to avoid temperature effects on the excess vaccine. At the same time, thermoelectric storage devices can be equipped with thermocouples to monitor internal temperatures, preventing vaccines from damage. Therefore, TEDs offer an efficient solution to the problem of storing and transporting vaccines [145].

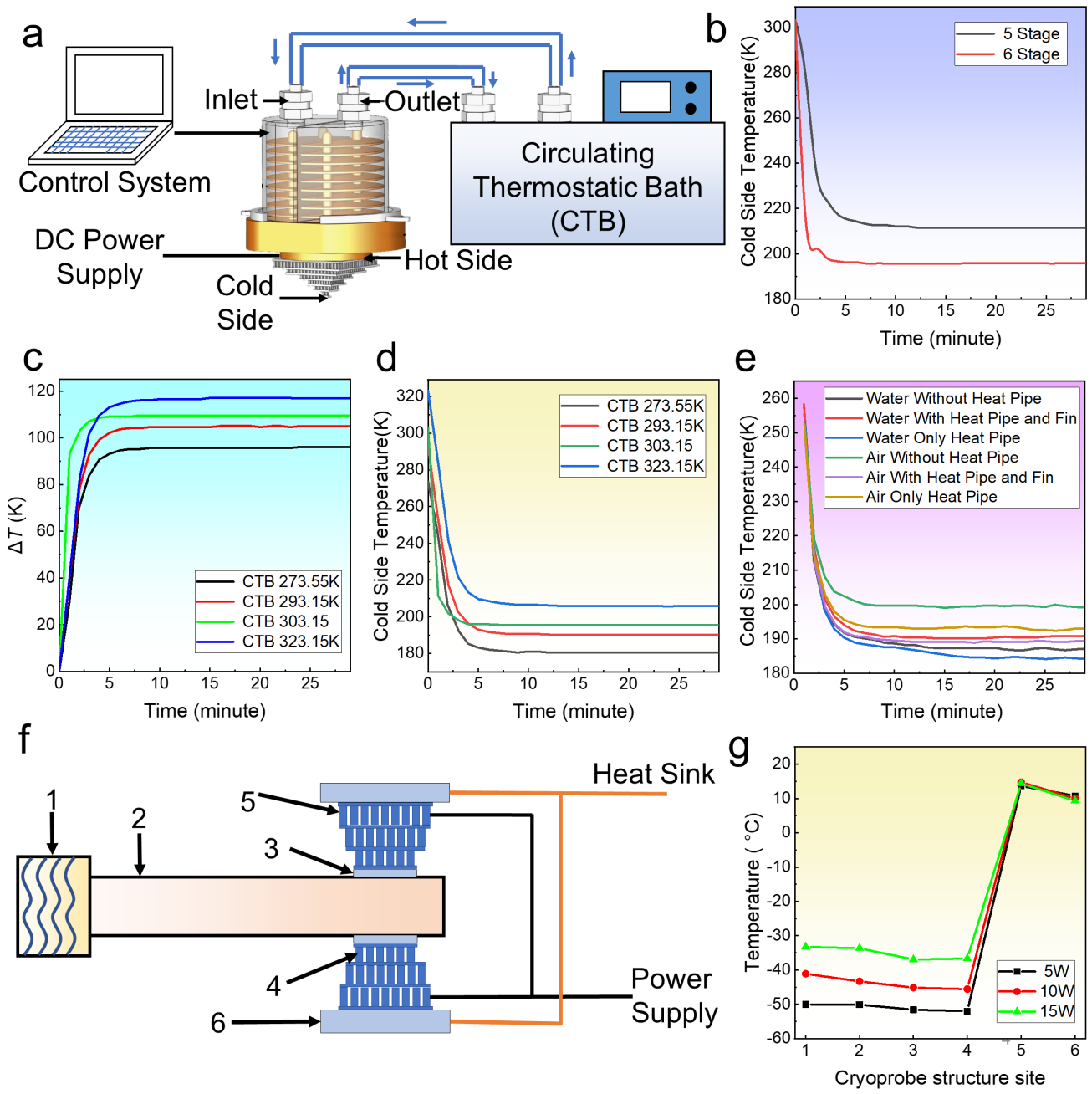

Figure 5 a) Diagram of a cryoprobe for cryosurgery. b) Cold side temperature at 5 and 6 thermoelectric cooler (TEC) levels. c) ΔT of the cryoprobe when the circulating thermostatic bath (CTB) is at different temperatures. d) Cold side temperature of the cryoprobe when the CTB is at different temperatures. e) Cold side temperature under different heat sink conditions. Reproduced with permission [16]. Copyright 2010, Elsevier. f) Diagram of a cryoprobe for cooling with the aid of a heat pipe, 1 is the tip of the probe, 2 is the heat pipe, 3 is the contact between the TEC module and the heat pipe, 4 is the cold side of the TEC module, 5 is the hot side of the TEC module and 6 is the contact between the

TEC module and the heat sink. g) Temperature of the cryoprobe at different positions. Reproduced with permission [12]. Copyright 1993, Taylor & Francis Group.

3.1.4 Skin cooler

In the case of acute soft tissue injuries such as sprains and strains, the patient should start applying icepacks as soon as possible to suppress inflammation [22]. Depending on the injury degree, it should be cooled for a maximum of 48 to 72 hours [22, 146-148]. Conventional treatments include immersion in ice water, cold application of cold gel, or the use of the freezing spray. However, these methods are difficult to treat patients with long-term continuous cryotherapy, and the long-term exposure of the body to cold temperatures can lead to secondary damage [149-151]. A cooling device with TECs as the core component is perfectly suited to this task as it allows quick switching between heating and cooling functions and requires little maintenance after the operation.

There are two main types of TECs for skin cooling, the first being cooling devices coupled to conventional ice pack cooling. **Figure 6a** shows a photograph of the TEC consisting of a 4 cm × 4 cm thermoelectric module, which can support a maximum voltage of 15.2 V and generate a maximum ΔT of 70 °C [22]. Such a TEC can be installed on the ice pack, and the cooling fluid inside the ice pack is directly cooled, allowing a uniform reduction in temperature at the injury site [22]. A temperature detector and oscillator can be inserted into the ice pack to facilitate accurate measurement of the ice pack temperature [22]. The device is also equipped with an electronic board and a heat sink. The electronic board is connected to the operating system, which allows the temperature of the ice pack to be instantly controlled [22]. The device is waterproofed with plastic welds and varnish [22]. Because of its low maximum voltage of only 15.2 V, it can be used in ambulances. When performing cryotherapy, the skin temperature should be quickly reduced to 5 °C, and rewarmed on the treatment to avoid tissue frostbite [152].

Figure 6b shows a comparison of the cooling effect of the TEC Smart Ice Pack with that of a

conventional ice pack. After 15 minutes of operation, the TEC Smart Ice Pack stabilizes at 5 °C, with the temperature range becoming progressively smaller as the running time increases. [22]. In contrast, the conventional ice packs, which start at a lower temperature, start to warm up after 13 minutes of operation and reach 19 °C at 200 minutes, which is no longer therapeutic and should be considered for replacement at 20 to 30 minutes [22]. The TEC Smart Ice Pack, which can be also operated automatically by the system, allows the temperature and cooling rate to be better adjusted to patients with different physical conditions [22].

The second type of TEC for skin cooling is the one that directly contacts the skin through the cooling head. Two different cooling heads for TECs exit. **Figure 6c** shows the point head and **Figure 6d** shows the sheet head. Both of them are designed with the cold side of the thermoelectric module connected to the aluminium head of the cooling head, and the hot side connected to the water cooling [129]. A temperature sensor can be added to the top of the cooling head to reduce the cooling error [129]. As can be seen, by an operating power of 50 W, the sheet head starts cooling the human skin more quickly but the subsequent cooling is more gradual, whereas the point head starts cooling at about 50 seconds but the skin cools quickly to below 10 °C [129]. It is easy to see that different cooling heads have different effects on the cooling rate, and that better treatment results can be achieved by changing the cooling head to suit the patient's different injuries and physical conditions.

Both above TECs are equipped with a large heat sink to support them for long periods of operation. However, for patients with less severe injuries or multiple sclerosis patients, who often do not need continuous cooling for so long, the portability of the device is more suitable [18]. For these patients, phase change materials (PCMs) with high heat storage density can be used instead of conventional water and air cooling [18]. **Figure 6e** shows TECs with PCMs for the heat sink. The hot side of its thermoelectric module is in direct contact with a 160 mm × 30 mm × 17.5 mm container storing PCMs, while the cold side is in contact with a water container that simulates a human arm with the same

volume as a PCM water container [18]. A thermal paste is used to enhance the thermal contact between the containers and the thermoelectric module [18]. Thermocouples are also inserted in both containers to monitor their temperature change [18]. To determine the heat dissipation effect of PCMs. Three different PCMs and three different voltages were used for the experiments. **Figure 6f** shows the cooling effect of the device with three different PCMs. As can be seen, among the three different PCMs at 6 W, HS34 that is a chemical-based PCM with a melting temperature of 36 °C and a freezing temperature of 36 °C has the best cooling effect and can be stabilized at 8 °C for a long time, while OM46 that is a bio-based PCM with a melting temperature of 48 °C and a freezing temperature of 45 °C has the worst performance [18]. The PCM-HS34 was then used to cool down the water at 3 W, 6 W, and 9 W. The results are shown in **Figure 6g**. At 3 W, the water was cooled to a minimum of 10 °C for 18 minutes, and at 6 W the water was cooled to a minimum of 8 °C for 12 minutes [18]. However, at 9 W, the water was cooled down to 8 °C and then raised quickly [18]. This is because at 9 W the PCM melts rapidly and loses its cooling effect. **Figure 6h** shows the temperature variation of the PCM at different power levels. When the water is cooled down to 8 °C, the PCM is already close to 40 °C. Yet, the maximum temperature of the PCM at 6 W is still less than 40 °C [18]. Therefore, it can be concluded that due to the nature of PCMs, the power of the TEC applying PCM cooling cannot be too high, limiting the range of TECs that can be used with PCMs cooling. If PCMs with better heat absorption could be developed, the working hours of such TECs would be greatly increased.

Fever patch is also a potential use for skin cooling. Considering the important factors of room-temperature thermoelectric performance, low toxicity, cost-effectiveness, and stability, Bi_2Te_3-based, MgAgSb-based, and PEDOT:PSS-based thermoelectric materials are popular [31, 32]. Among them, Bi_2Te_3-based materials show the best room-temperature performance with high cost-effectiveness [31]. MgAgSb-based materials have experimental *ZT* values of up to 0.7 at room temperature [153],

showing great potential in fever patches with lower cost and with higher safety [32]. PEDOT:PSS-based materials have excellent, and have been considered as alternative materials for fever patches [71].

Fever patches currently available are composed mainly of hydrogels. Hydrogels are efficient in cooling, but cannot be used repeatedly and require regular manual replacement. A TED could be designed for fever reduction by incorporating thermocouples to real-time monitor the temperature of patients. Moreover, a digital system with TEGs at the hot side to recycle waste heat can be efficiently used to reduce the temperature of patients and decrease the power requirements of the device [154].

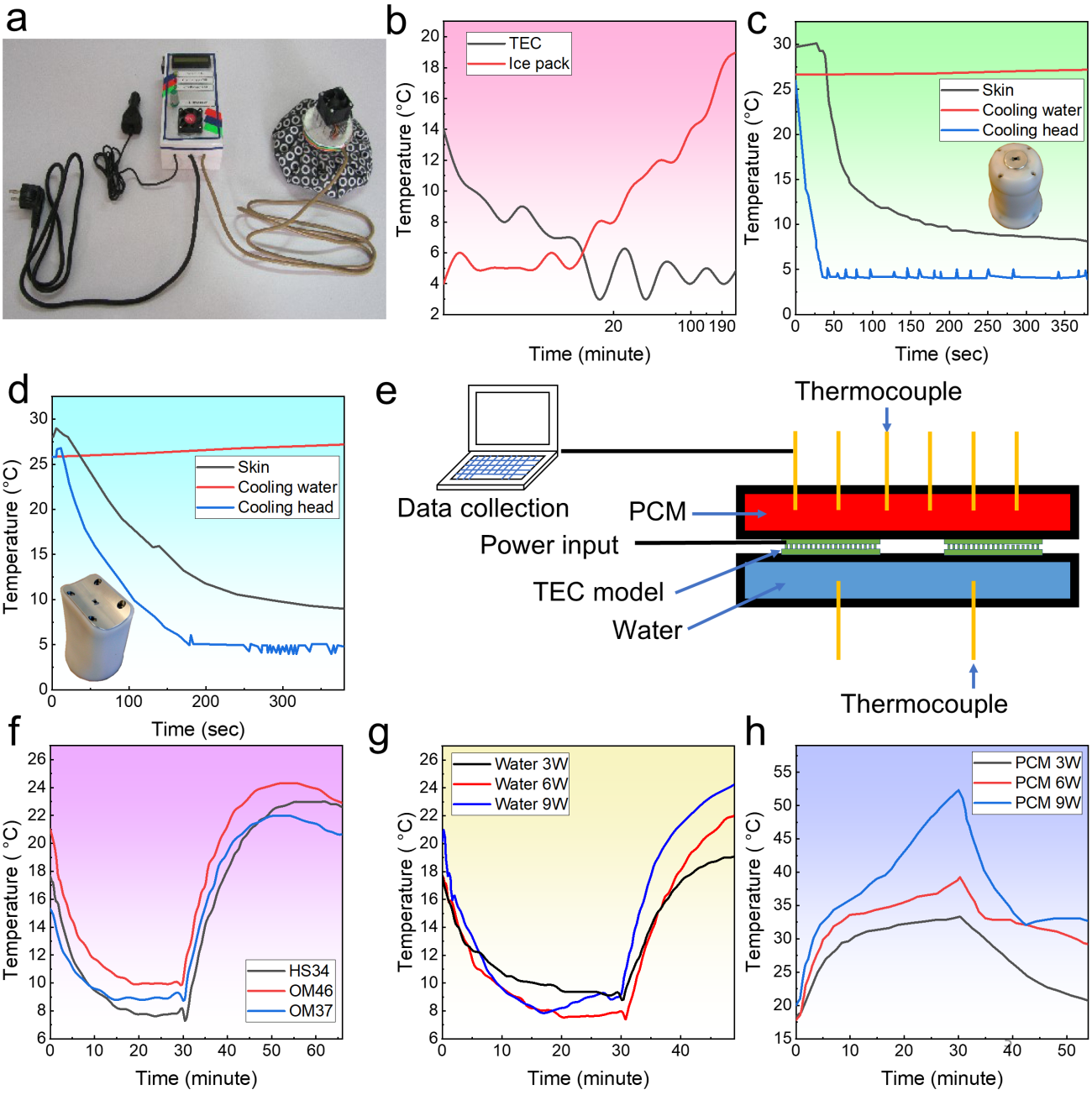

Figure 6 a) Diagram of a thermoelectric cooler (TEC) Smart Ice Pack. b) Comparison of the cooling performance of a TEC Smart Ice Pack against a conventional ice pack. Reproduced under a Creative Commons Attribution-NonCommercial 4.0 International License [22]. Copyright 2018, IIUM Press. c) Cooling effect of a point head TEC. d) Cooling effect of a sheet head TEC. Reproduced with permission [129]. Copyright 2018, Elsevier. e) Diagram of a TEC device with phase change material (PCM) cooling. f) Temperature of water at different PCM. g) Temperature of water at different power. H) Temperature of the PCM at different power. Reproduced with permission [18]. Copyright 2014,

Elsevier.

3.2 Thermoelectric generators

In addition to TECs, TEGs can also be used for medical applications, which can be divided into implantable TEGs and wearable TEGs.

3.2.1 Implantable thermoelectric generators

IMDs have been used in medical applications since 1958 [10]. The lifespan of IMDs has been shortened because of limitations in battery technology and patients must replace their batteries with surgery every 10 years [10, 26, 155]. This undoubtedly increases the pain and financial strain on patients [10]. TEGs were used in the early 1970s as part of a nuclear battery for IMDs, but were abandoned as a result of the dangers of the radioactive material [10, 26].

Nowadays, with the development of thermoelectric technology, TEGs can generate electricity directly from human body temperature instead of using nuclear heat, which illustrates the potential of using TEGs to drive IMDs [130]. For implantable TEGs, the implantation site needs to ensure that the thermoelectric module has a maximum ΔT. The exact implantation location is shown in **Figure 7a**, where the thermoelectric module has dimensions of 20 mm × 20 mm × 3 mm [130]. Using the Pennes biothermal equation, it can be calculated that the implantation site with the maximum ΔT should be as close to the surface skin as possible [130]. In order to clarify the optimal location, five different trials were carried out in close proximity to the superficial skin (**Figure 7b**) [130]. The ΔT increased to 0.482 K at 7 cm when the TEGs were implanted further away from the body core, and the isotherms were distorted because TEGs had different thermal properties to the human body.

Different ambient temperatures and heat transfer coefficients affect the cold and hot side temperatures of the TED (**Figure 7c**) [130]. Five different sets of ambient temperature measurements were carried out at three different heat transfer coefficients of 10 $Wm^{-2}K^{-1}$, 20 $Wm^{-2}K^{-1}$, and 50 $Wm^{-2}K^{-1}$ [130]. When heat transfer coefficients are the same, a lower ambient temperature means a higher

ΔT; while at the same ambient temperatures, a higher heat transfer coefficient results in a higher ambient temperature, with a maximum ΔT of 1.142 K at 273 K TA. [130]. If the heat transfer strategy can be further optimised, the ΔT can be further increased. Since the implanted TEGs generate electricity directly from the human body temperature, the physiological state of the human body is also a factor that can effectively influence the ΔT. The body's blood perfusion and metabolic heat are different under different physiological activities [130]. **Figure 7d** shows the ΔT of TEGs for different blood perfusion scenarios. When the blood perfusion increases, the ΔT of TEGs increases [130]. At a metabolic heat of 42,000 Wm^{-3} and blood perfusion of 0.05 $mls^{-1}ml^{-1}$, the ΔT can be as high as 0.95 K at this point [130]. When the TEGs are inserted into the pork simulating human body temperature, the ΔT is stable at around 0.5 K and the output voltage is around 3.3 mV [130]. If the surface of the pork is cooled, the output voltage can reach 6 mV [130]. To further increase the performance of the implanted TEGs, multi-stage TEGs were used instead of single-stage TEGs. 3-stage TEGs were constructed by combining three 10 mm × 10 mm × 3.9 mm TEGs [130]. The results of the experiments conducted are shown in **Figure 7e** [130]. As the implantation time increased, ΔT eventually stabilized at 1.3 K with a voltage of 2.9 mV [130]. At 100 minutes, the maximum output voltage was 11 mV, which was sufficient for the IMD, when cooling of the pork surface began [130].

Animal experiments in rabbits can further clarify the performance of the implanted TEGs. By increasing the voltage output of the TEGs through a boost circuit, the IMDs can be better powered The results are shown in **Figure 7f** [25]. When the rabbits are first implanted, ΔT is large because the temperature rises at different rates on each side of the device. However, after the temperature has stabilized, ΔT is 1.1K [25]. The output voltage did not change too much throughout, with the aid of the boost circuit, and remained at around 3.3 V [25]. By placing the single-stage TEGs in a perfect position, the maximum output function can be measured to be about 0.027 mW with an open-circuit voltage of 18.9 mV (**Figure 7g**) [25]. If multi-stage TEGs are used, the ΔT increases because of the

increase in thickness. A comparison of the performance from single-stage to 4-stage TEGs is shown in **Figure 7h** [25]. Although the output voltage and power increas with the number of stages, it is not a proportional growth. Combined with the limited volume of the human body, the number of stages cannot be increased indefinitely and the optimum number of TEG stages needs to be considered [25]. Today IMDs require less voltage and therefore implantable TEGs can meet their needs [130]. When TEGs are implanted directly into the body, they can cause symptoms such as allergies and need to be wrapped in PDMS, which reduces the performance of TEGs. Therefore, better wrapping strategies need to be developed for further improvement. At the same time, most research on thermoelectric materials has focused on improving the thermoelectric properties, but the mechanical properties of the materials are also important. Particularly, failure materials inside the body for implantable TEDs can result in direct exposure of the electronic components to the body, which may lead to allergic or toxic reactions that can cause damage to the body. Extensive investigations have been proposed to improve the mechanical properties of thermoelectric materials. For example, Re-doping can significantly increase the Vickers microhardness of GeTe [156]. The preparation processes of materials also affect their mechanical properties. For example, hot-pressing can be used to create dense, brittle, and hard thermoelectric materials, while the materials prepared by cold-pressing have low densities, weak mechanical properties, and high resistivities [1]. Rational structural and dimensional design of thermoelectric materials and devices can also improve their mechanical properties [1]. Moreover, new nanoindentation techniques have been developed to investigate the mechanical properties of materials and devices for ensuring that implantable medical TEDs have the right mechanical properties to avoid accidents during implantation [1, 156]. Biocompatibility is another important factor for the implantation of TEDs. Machine learning combined with high-throughput theoretical predictions and

high-throughput experiments allow the optimization of existing thermoelectric materials and the discovery of new biocompatible thermoelectric materials [157].

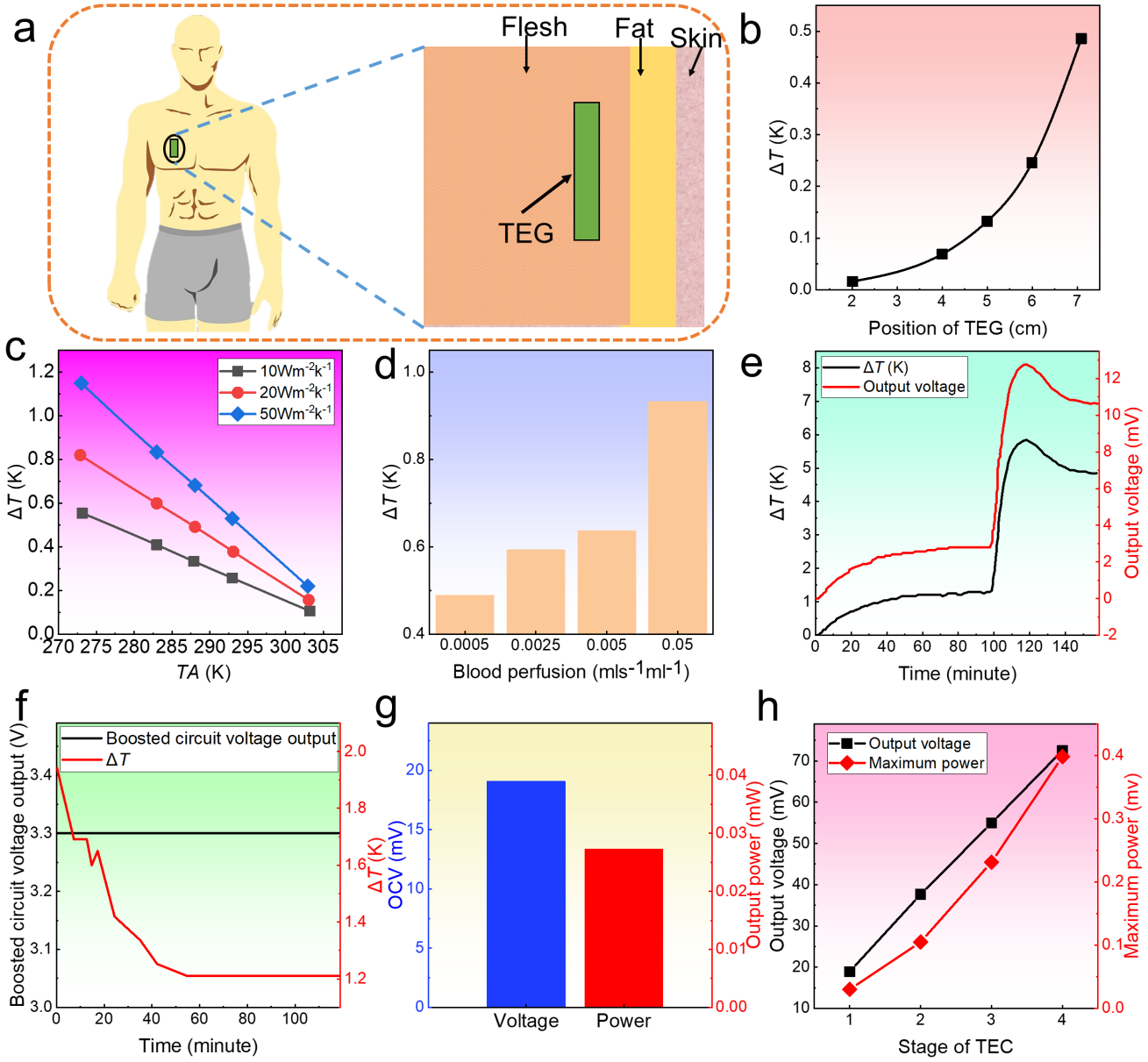

Figure 7 a) Conceptual diagram of the implantation of an implantable thermoelectric generator (TEG). b) Temperature difference (ΔT) at different implantation locations. c) ΔT at different environmental temperatures and different heat transfer coefficients. d) ΔT at different blood perfusion scenarios. e) Voltage and ΔT of the device output after cooling the body surface. Reproduced with permission [130]. Copyright 2007, IOP Publishing. f) Voltage and ΔT of the device output with the aid of a boost circuit. g) Voltage and power output of the device. h) Voltage and power output of the appliance at different

stages. Reproduced with permission [25]. Copyright 2014, The American Society of Mechanical Engineers.

3.2.2 Wearable thermoelectric generators

With the advances in medical technology, in addition to the increasing use of IMDs, the growing demand is to develop various medical sensors for monitoring the physiological state of patients [10]. Newly developed microelectromechanical systems enable operating these medical sensors with a very low power supply from a few microwatts to a few milliwatts [105, 158]. To increase the portability of this type of medical device, it can be combined with wearable TEGs to power up at any time [28].

Common wearable TEGs can be divided into organic flexible TEGs and inorganic bulk flexible TEGs. Organic materials are more flexible and comfortable than inorganic materials. However, because of the lower $S^2\sigma$ of organic materials, it is difficult to ensure the stable and long-lasting operation of the sensor [32]. To ensure that the sensor can be always operated, most of the wearable TEGs used in the medical field are inorganic bulk TEGs. To overcome the poor flexibility and low wearability of inorganic bulk materials, flexible substrates, such as thermal interface layers (TILs), and PDMS can be used to adapt to the human surface, improving the flexibility and wearability of TEG devices [105]. **Figure 8a** shows a diagram of wearable TEGs for the human wrist [105]. The main structure is a number of n- and p-type thermoelectric legs, interconnected by copper strips and encapsulated by PDMS, with a thin layer of TIL made of silicone rubber on the bottom [105]. As the TIL was deformed, the temperature distribution on the TED was not uniform, as shown in **Figure 8b** [105]. The ΔT is symmetrical along the left and right sides of the TEG, with ΔT as high as 0.32 K in the PDMS region on both sides of the device and only 0.19 K in the core region containing the TE legs, due to the relatively low κ in the PDMS and the large amount of heat transferred along the copper strip to the core region [105]. This allows a large amount of heat to avoid the PDMS and to flow through the TE leg for enhancing the heat collection in the TEGs [105].

In order to investigate the bending effect of the wearable TEGs on the performance, a comparison was made between TEGs laminated to a curved surface with a radius of curvature of R = 10 mm and 30 mm, and TEGs laminated to a flat surface [105]. The difference in ΔT is only 0.002 K when the device is operated on R = 10 mm and on a flat surface, which indicates that the radius of curvature has no effect on the performance of the TEGs [105]. The thickness and deformation of the TILs may also influence the performance of the TEGs. The ΔT between three groups of TEGs with different thicknesses of TILs were examined and found to increase with increasing the thickness, as shown in **Figure 8c** [105]. At the same time, if the TIL is too thick, the TIL results in a large heat loss and leads to a lower final output voltage [105]. Therefore, the TIL should be selected at a suitable thickness to balance the heat flow distance from the skin to the environment with the heat loss from the TIL. For wearable TEGs, the cold side is dissipated by the ambient temperature, and if the wearer starts to walk around, then air convection is enhanced, which increases the heat dissipation to the cold side [105]. **Figure 8d** shows the voltage variation of the TEGs when walking and standing. As can be seen, the output voltage is only about 3 mV when the wearer remains standing still for the first 20 seconds; but when the wearer starts to walk, the output voltage increases to 11.2 mV due to enhanced air convection [105]. When combined with a boost converter, this can be further stabilized and enhanced [105, 159].

Because the thermoelectric leg is in direct contact with the TIL, heat needs to flow across the TIL laterally before the heat can be utilized by the TE leg, as illustrated in **Figure 8e** [24]. During this process, the heat from the TIL diffuses into the media surrounding the thermoelectric leg. In terms of flexible TEGs, these elastomers can cause a significant degradation in the performance of TEGs [24]. The thermal resistance of the thermoelectric module can affect the performance of the TEGs. **Figure 8f** displays an optical image, showing a wearable TEG with a leg length of 2.2 mm [24]. To enhance the performance, the fill factor (FF) should be reduced by reducing the number of thermoelectric legs or reducing their base area to increase their thermal resistance [24]. At a κ of 1.5 W m^{-1} K^{-1}, the TEGs reach a maximum power with the FF of 3%. When there are 10 thermoelectric legs, and the power

decreases rapidly with increasing the FF, as shown in **Figure 8g** [24]. The highest power can be achieved at the FF of ~25 at the κ of 0.2 W m^{-1} K^{-1}, where the number of TE legs approaches 100 [24]. Although there is a similar optimum power for all three different κ, it is extremely difficult to manufacture TEGs with the FF of less than 20 due to the manufacturing process. Therefore, a balance needs to be found between κ, performance, and the manufacturing process [24]. The different leg lengths of the thermoelectric legs can also affect the performance (**Figure 8h**) [24]. The power of both custom-made thermoelectric modules and commercial off-the-shelf (COTS) thermoelectric modules increases with increasing leg length, while their power density shows an opposite trend [24]. Therefore, it is essential to choose the right thermoelectric leg length and TIL thickness. For wearable TEGs, the air velocity in different environments also affects the performance of TEGs [24]. The saturation output power was measured for wrist TEGs with and without a heat sink at a human core temperature of 37 °C and an ambient temperature of 22.6 °C [24]. The experimental results show an increase in output power for both as the air velocity increases, when the output power of the TEGs with the heat sink increases from 20 μW to nearly 120 μW as the air velocity increases from 0 to 0.8 m/s. This result is similar to the previous experiment where walking would improve device performance [24, 105]. The maximum output of TEGs with a heat sink can be four times higher than that without a heat sink, indicating the need for a heat sink for wearable TEGs [24]. The performance of TEGs can be further improved if oversized heat sinks can be solved.

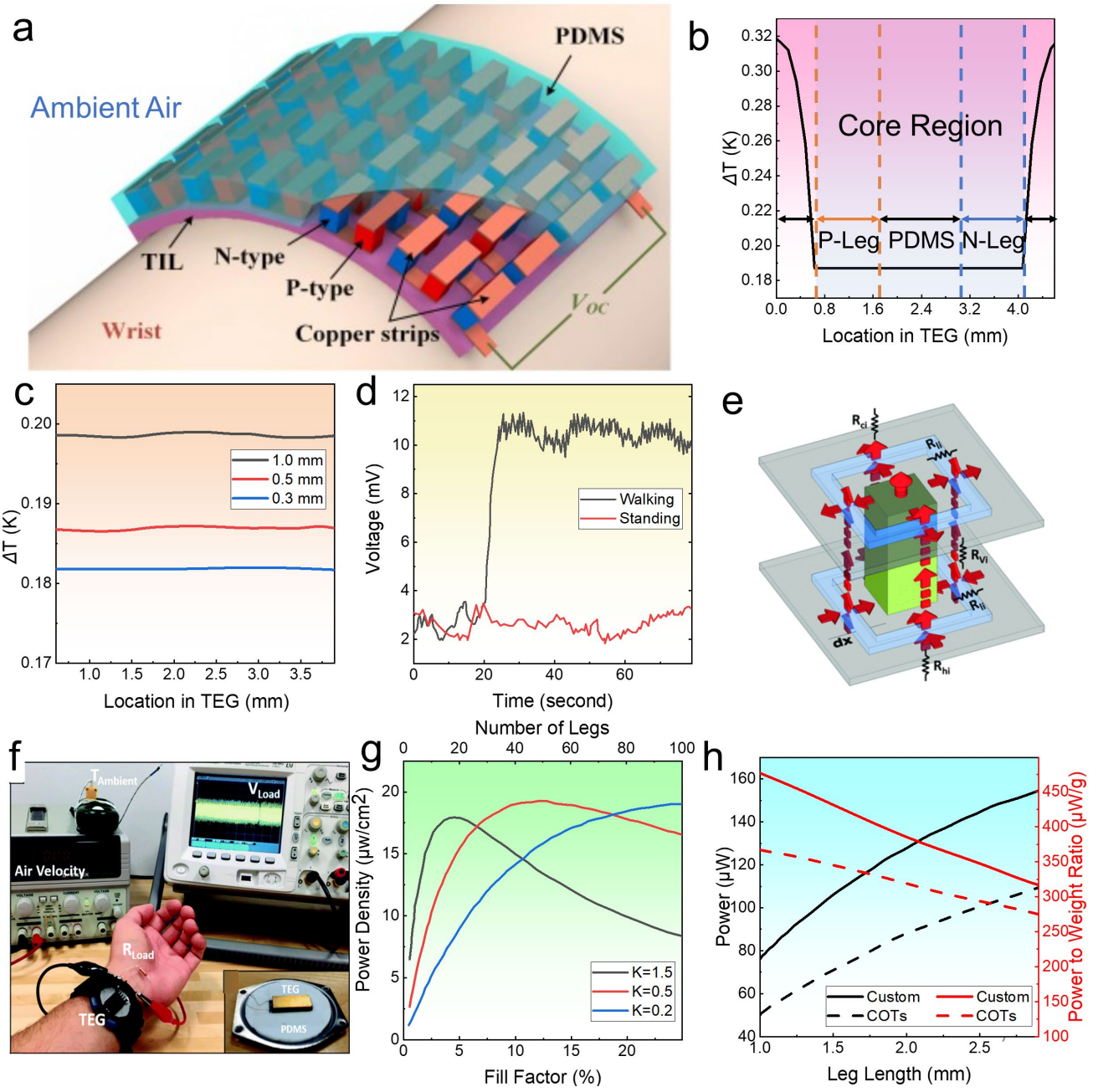

Figure 8 a) Conceptual diagram of a wearable thermoelectric generator (TEG). b) Temperature difference (ΔT) between different positions of a TEG. c) ΔT between different positions of a TEG at different TIL thicknesses. d) Voltage output of a TEG in the wearer's walking and standing states. Reproduced with permission [105]. Copyright 2017, Elsevier. e) Schematic diagram of heat transfer in the TE leg. f) Finished diagram of a wearable TEG device. g) Power density at different fill factors. h) Power and power to weight ratio differences between custom and commercial off-the-shelf (COTS) devices at different leg lengths. Reproduced with permission [24]. Copyright 2016, Royal Society of

Chemistry.

4 Conclusions, challenges, and outlooks

Thermoelectric materials and their devices can realize the direct conversion between heat and electricity, therefore can act as practical devices for localized power generation and refrigeration. Based on these unique functions, thermoelectrics devices are good candidates with great potential for employing in the medication field, such as hospitals, ambulances, and patient homes. With the rapid development of thermoelectric science and technology, TECs have been started to be used in cryotherapy to suppress inflammation, remove pathological tissue, control brain signal strength, and improve wound recovery [160]. As well, TECs were proved to be effective to prevent patients from dying from cerebral hypoxia through CCH, treat chronic diseases such as epilepsy by suppressing brain waves when installed in the brain, and reduce post-operative scarring. TECs for skin cooling also allow long-term cooling of patients and avoid frostbite. In terms of TEGs, they are still at the very beginning stage. Implantable TEGs use the body temperature to supply energy to IMDs for a long and stable period in the human body, increasing the life of IMDs. The wearable TEGs can be charged with a biomedical sensor using the difference in temperature between the human body and the environment, so that the patient can real-time monitor their body status. Therefore, there has been significant progress in the application of thermoelectrics in medication.

It should be noted that there are still considerable challenges in the research of thermoelectrics for medical applications. The most significant challenge is the unsatisfied ZT value for thermoelectric material. According to **Formula 3**, the magnitude of the ZT value determines the performance of TEDs. Extensive efforts have been made to enhance ZT value by coupling S, σ, and κ. Band engineering by doping or vacancy tuning can tune S and σ to optimize the $S^2\sigma$ [161]. Energy filtering can be used to increase the S while keeping the σ by introducing rational nanoinclusions [162, 163], while suppressing

the κ can be realized by structure engineering [164]. Currently, thermoelectric materials still have difficulties in achieving *ZT* values above 1.5 at room temperature [32], which is difficult to match with the medical application environment, meanwhile considering the heat sink, ΔT of TEDs, long-term stable and efficient operation is still a challenge for medical TEDs [165, 166]. This is further limited by the fact that Bi_2Te_3 is often covered with a biocompatible material such as PDMS, with the aim to cope with the biocompatibility issues. These covers may reduce the thermoelectric conversion efficiency of the materials and devices. Meanwhile, in order to increase portability, the small size of the device makes it difficult to increase performance and hence cannot be used in many large medical devices and some power-hungry IMDs. In the case of TECs, higher power is often used to compensate for the performance deficit. For ambulances or patients who need to use TEC devices for long periods of time, running nearly 300 W for long periods of time is bound to become an unaffordable burden, while the high cost of Bi_2Te_3 results in higher costs for TE devices. The large size and weight of the heat sink are also challenge for thermoelectric devices, especially for TECs. To ensure that the TECs are cooled effectively, the temperature at the hot side must be controlled. This results in TEDs often being paired with larger volumes of water or air cooling. Moreover, the noise of air cooling and the low portability of water-cooling conflict with the advantages of no noise and high portability of thermoelectric materials. PCM avoids these problems but does not provide stable cooling of the hot side of the device in the long term. For TEGs, environmental factors can greatly affect performance. In some regions, temperatures can reach 40 °C in summer, when the ΔT between the human body and the environment is low, and the performance of TEGs can be significantly inhibited or unable to meet demand. In these areas, because of the high temperature, people tend to choose cooling devices such as air conditioners for indoor cooling, leading to an increase in the greenhouse effect. Commercial

TECs have a carbon-neutral capability for green buildings due to the zero-emission advantage of TEDs [167]. By integration with photovoltaics, photovoltaic panels can be used to convert solar energy into electricity to be supplied to TEDs. TECs can be used to cool the supply air duct to provide cooling air, while the air duct is placed close to the hot side of the TECs to dissipate heat [167, 168]. In winter, the heating function can be performed by switching the direction of the current [167, 168]. Only the ventilation system requires an additional energy supply, and the carbon footprint of the whole system is far less than that of conventional cooling methods [167]. An additional solar condensate system can also be built on the system to alleviate the high demand for water in tropical regions [167]. TEDs can be used as personal thermal management devices in these areas. A recent study shows that thermoelectric fabrics can use ambient and body temperatures to cool as well as generate electricity in an integrated cycle [169], which offers a potential solution for harvesting energy from the outside world and the human body for passive thermal management, and can additionally power electronic devices with low power consumption [169]. Flexible thermoelectric materials offer the potential for continuous green energy solutions, but are currently not widely available commercially due to their low performance and high cost, which is a challenge that needs to be addressed [169].

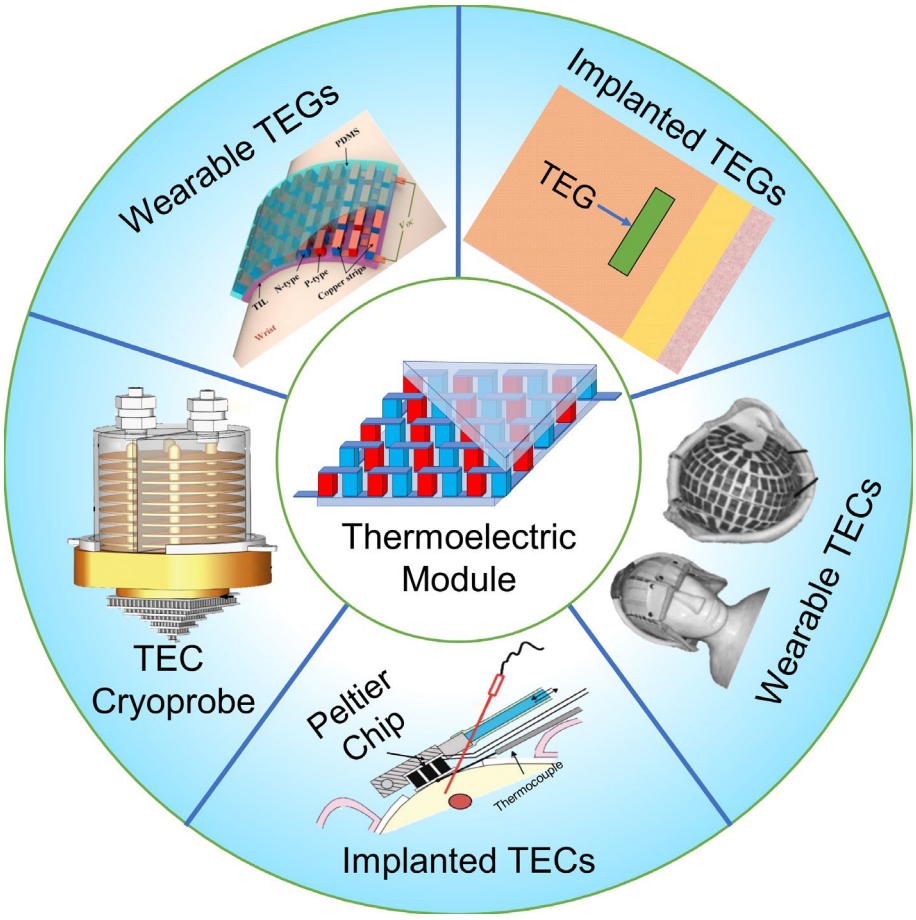

Figure 9 Prospects for TE materials in medical applications for wearable TEG devices, implantable TEG devices, wearable TEC devices, implantable TEC devices, TECs cryoprobes. Wearable TEC, reproduced with permission [14]. Copyright 2008, Taylor & Francis Group. Implantable TEC, reproduced with permission [107]. Copyright 2010, J-STAGE. TEC cryoprobe, reproduced with permission [16]. Copyright 2010, Elsevier. Implantable TEG, reproduced with permission [130]. Copyright 2007, IOP Publishing. Wearable TEGs, reproduced with permission [105]. Copyright 2017, Elsevier. Thermoelectric module, reproduced with permission [1]. Copyright 2020, American Chemical Society.

In terms of the outlooks for further optimizing TEDs, a few perspectives are proposed here:

1) **Improving the *ZT* values of thermoelectric materials.** For medical TEDs, the *ZT* values of thermoelectric materials at room temperature should be significantly improved by newly developed

strategies, such as rational band engineering, structural engineering, and advanced fabrication techniques. Very recently, new thermoelectric materials with high near-room-temperature performance such as SnSe crystals and MgAgSb are developing [1, 32, 170, 171]. As well, non-toxic and high-stability thermoelectric materials need to be developed to better fit the human body and different application scenarios. Particularly, the fabrication of medication-suitable thermoelectric materials on an industrial scale is critically important.

2) **Improving device performance and stability by optimizing device design.** Many factors affect the design of medical-use thermoelectric devices, such as rational fill factors, dimensions, substrates, electrodes, fillers, and wires. The topological design is a key factor to optimize the performance of the device. For example, the air has less influence than PDMS [24], and device performance can be enhanced by doping the TIL with different materials. Besides, to increase the biocompatibility of the medical TEDs, new materials should be developed to replace PDMS or new designs can be optimized with other materials to reduce the thickness of PDMS to increase device performance. For implantable miniature TEDs, the effectiveness of the device should be further enhanced. By installing multiple thermoelectric modules around the target location, they work together to optimize the performance of the device. Improved device design can extend the benefits of TEDs, such as improving the cryoprobe head to avoid allergy by allowing the device to cool and remove the target tissue without direct contact to Jeanette. It also further reduces scarring and meets the need for minimally invasive procedures. 3D printing technology is becoming increasingly sophisticated and allows the manufacturing of devices with complex shapes and aspect ratios to overcome the limitations of materials with high κ [33, 172]. 3D printing technology can simplify the manufacturing of complex thermoelectric devices, which can facilitate the commercialization of medical TEDs [33].

3) **Optimize the accessories**. TECs need to keep a stable low temperature at their hot sides, therefore the heat sink should be well designed with both high heat dissipation, low weight, and high stability. Developing a high-flexibility and high-performing heat sink is a promising direction for TECs that

target medication use. As well, for TECs that require water cooling to sink, a split design can be used to place the water-cooling unit separately to reduce noise impact, while adding a swivel to the bed or wall for storing and releasing the water pipes to increase the portability of the device. For larger TEC devices, install a TEG model on the hot side to use the excess heat to generate electricity and ease the demand on the power supply.

4) **Combination with other functional materials and devices**. To increase the stability of the output of the TEGs, it can be combined with a battery, solar cell, or supercapacitor to allow TEGs to continue to generate electricity and charge the battery or capacitor even when it is not outputting, which can ensure that the medical device in use can be supplied with energy consistently over time. For wearable TEGs, different designs can be used depending on the ambient temperature. For example, in winter the hot side is close to the body and in summer the cold side is close to the body to reduce the environmental impact on the device. TEDs can also be used in smart textiles [90]. Smart textiles can provide a continuous energy supply to wearable sensors by integrating with thermoelectric, photovoltaic, and piezoelectric devices [173, 174]. For example, the photothermal layer can further improve the performance of thermoelectric materials [174]. Therefore, combining TEDs with piezoelectric and photovoltaic technology is promising for development.

Acknowledgements

This work was financially supported by the Australian Research Council, HBIS-UQ Innovation Centre for Sustainable Steel project, and QUT Capacity Building Professor Program. The authors thank T.Y.C and W.Y.C. for data collection.

Reference

[1] X.-L. Shi, J. Zou, Z.-G. Chen, Chem. Rev. 120 (15) (2020) 7399-7515.

[2] H.S. Kim, W. Liu, Z. Ren, Energy Environ. Sci. 10 (1) (2017) 69-85.

[3] P. Heremans Joseph, V. Jovovic, S. Toberer Eric, A. Saramat, K. Kurosaki, A. Charoenphakdee, S. Yamanaka, G.J. Snyder, Science 321 (5888) (2008) 554-557.

[4] M. Hong, Z.-G. Chen, J. Zou, Chin. Phys. B 27 (4) (2018) 048403.

[5] D. Zhao, G. Tan, Appl. Therm. Eng. 66 (1) (2014) 15-24.

[6] S. Sharma, V.K. Dwivedi, S.N. Pandit, Int. J. Green Energy 11 (9) (2014) 899-909.

[7] X.-L. Shi, W.-Y. Chen, T. Zhang, J. Zou, Z.-G. Chen, Energy Environ. Sci. 14 (2) (2021) 729-764.

[8] S. Chatterjee, Int. J. Eng. Res. Appl. 3 (2013) 2029-2032.

[9] R.C. O'Brien, R.M. Ambrosi, N.P. Bannister, S.D. Howe, H.V. Atkinson, J. Nucl. Mater. 377 (3) (2008) 506-521.

[10] Kumar, J.b. Veluru, Subramanian, A. Bandla, Thakor, Ramakrishna, W. he, Designs 3 (2019) 22.

[11] A. Chen, P.K. Wright, Medical applications of thermoelectrics, 2012.

[12] A. Hamilton, J. Hu, J. Med. Eng. Technol. 17 (3) (1993) 104-109.

[13] L.I. Anatychuk, N.V. Pasechnikova, V.O. Naumenko, O.S. Zadorozhnyi, S.L. Danyliuk, M.V. Havryliukйй, V.A. Tiumentsev, R.R. Kobylianskyi, Phys. Solid State 21 (1) (2020) 140-145.

[14] R. Ahiska, A.H. Yavuz, M. Kaymaz, İ. Güler, Instrum. Sci. Technol. 36 (6) (2008) 636-655.

[15] M. Kapıdere, R. Ahıska, İ. Güler, J. Med. Syst. 29 (5) (2005) 501-512.

[16] N. Putra, Ardiyansyah, W. Sukyono, D. Johansen, F.N. Iskandar, Cryogenics 50 (11) (2010) 759-764.

[17] K. Morizane, T. Ogata, T. Morino, H. Horiuchi, G. Yamaoka, M. Hino, H. Miura, Neurosci. Res.

72 (3) (2012) 279-282.

[18] X. Li, S. Mahmoud, R.K. Al-Dadah, A. Elsayed, Energy Procedia 61 (2014) 2399-2402.

[19] N. Mejia, K. Dedow, L. Nguy, P. Sullivan, S. Khoshnevis, K.R. Diller, J. Med. Devices 9 (4) (2015) 0445021-0445026.

[20] F.A. Barber, Am. J. Knee Surg. 13 (2) (2000) 97-102.

[21] R. Waugh, E.A. Evans, Biophys. J. 26 (1) (1979) 115-131.

[22] K. Naser, R. Abbas, P.R.H. Reza, IIUM Eng. J. 19 (1) (2018) 117-128.

[23] D. Feng, C. Jiang, G. Lim, L.J. Cimini, G. Feng, G.Y. Li, IEEE Commun. Surv. Tutor. 15 (1) (2013) 167-178.

[24] F. Suarez, A. Nozariasbmarz, D. Vashaee, M.C. Öztürk, Energy Environ. Sci. 9 (6) (2016) 2099-2113.

[25] Y. Yang, G. Dong Xu, J. Liu, J. Med. Devices Trans. ASME. 8 (1) (2013) 014507.

[26] X. Wei, J. Liu, Front. Energy 2 (1) (2008) 1-13.

[27] V. Leonov, R.J.M. Vullers, J. Electron. Mater. 38 (7) (2009) 1491-1498.

[28] V. Leonov, Energy Harvesting for Self-Powered Wearable Devices, Springer, Boston, MA2011.

[29] C. Wood, Rep. Prog. Phys. 51 (4) (1988) 459-539.

[30] H. Lee, Energy 56 (2013) 61-69.

[31] J. Pei, B. Cai, H.-L. Zhuang, J.-F. Li, Natl. Sci. Rev. 7 (12) (2020) 1856-1858.

[32] Z. Soleimani, S. Zoras, B. Ceranic, S. Shahzad, Y. Cui, Sustain. Energy Technol. Assess. 37 (2020) 100604.

[33] N. Jia, J. Cao, X.Y. Tan, J. Dong, H. Liu, C.K.I. Tan, J. Xu, Q. Yan, X.J. Loh, A. Suwardi, Mater. Today Phys. 21 (2021) 100519.

[34] N. Jia, J. Cao, X.Y. Tan, J. Zheng, S.W. Chien, L. Yang, K. Chen, H.K. Ng, S.S. Faye Duran, H. Liu, C.K. Ivan Tan, Z. Li, J. Xu, J. Wu, Q. Yan, A. Suwardi, J. Mater. Chem. A 9 (41) (2021) 23335-23344.

[35] K. Kishimoto, M. Tsukamoto, T. Koyanagi, J. Appl. Phys. 92 (9) (2002) 5331-5339.

[36] D.S. Moran, L. Mendal, Sports Med. 32 (14) (2002) 879-885.

[37] B. Madavali, H.-S. Kim, K.-H. Lee, S.-J. Hong, Intermetallics 82 (2017) 68-75.

[38] B. Cao, J. Jian, B. Ge, S. Li, H. Wang, J. Liu, H. Zhao, Chin. Phys. B 26 (1) (2017) 017202.

[39] F. Hao, P. Qiu, Y. Tang, S. Bai, T. Xing, H.-S. Chu, Q. Zhang, P. Lu, T. Zhang, D. Ren, J. Chen, X. Shi, L. Chen, Energy Environ. Sci. 9 (10) (2016) 3120-3127.

[40] F. Serrano-Sánchez, M. Gharsallah, N.M. Nemes, N. Biskup, M. Varela, J.L. Martínez, M.T. Fernández-Díaz, J.A. Alonso, Sci. Rep. 7 (1) (2017) 6277.

[41] Y. Wang, W.-D. Liu, X.-L. Shi, M. Hong, L.-J. Wang, M. Li, H. Wang, J. Zou, Z.-G. Chen, Chem. Eng. J. 391 (2020) 123513.

[42] Y. Pei, H. Wang, G.J. Snyder, Adv. Mater. 24 (46) (2012) 6125-6135.

[43] S.I. Kim, K.H. Lee, H.A. Mun, H.S. Kim, S.W. Hwang, J.W. Roh, D.J. Yang, W.H. Shin, X.S. Li, Y.H. Lee, G.J. Snyder, S.W. Kim, Science 348 (6230) (2015) 109-114.

[44] L. Hu, H. Wu, T. Zhu, C. Fu, J. He, P. Ying, X. Zhao, Adv. Energy Mater. 5 (17) (2015) 1500411.

[45] X. Chen, H. Wu, J. Cui, Y. Xiao, Y. Zhang, J. He, Y. Chen, J. Cao, W. Cai, S.J. Pennycook, Z. Liu, L.-D. Zhao, J. Sui, Nano Energy 52 (2018) 246-255.

[46] J. Yu, C. Fu, Y. Liu, K. Xia, U. Aydemir, T.C. Chasapis, G.J. Snyder, X. Zhao, T. Zhu, Adv. Energy Mater. 8 (1) (2018) 1701313.

[47] J. Hwang, H. Kim, M.-K. Han, J. Hong, J.-H. Shim, J.-Y. Tak, Y.S. Lim, Y. Jin, J. Kim, H. Park,

D.-K. Lee, J.-H. Bahk, S.-J. Kim, W. Kim, ACS Nano 13 (7) (2019) 8347-8355.

[48] Y.F. Tsai, P.C. Wei, L. Chang, K.K. Wang, C.C. Yang, Y.C. Lai, C.R. Hsing, C.M. Wei, J. He, G.J. Snyder, H.J. Wu, Adv. Mater. 33 (1) (2021) 2170008.

[49] B. Qin, D. Wang, X. Liu, Y. Qin, J.-F. Dong, J. Luo, J.-W. Li, W. Liu, G. Tan, X. Tang, J.-F. Li, J. He, L.-D. Zhao, Science 373 (6554) (2021) 556-561.

[50] D. Yang, X. Su, J. Li, H. Bai, S. Wang, Z. Li, H. Tang, K. Tang, T. Luo, Y. Yan, J. Wu, J. Yang, Q. Zhang, C. Uher, M.G. Kanatzidis, X. Tang, Adv. Mater. (Weinheim, Ger.) 32 (40) (2020) 2003730.

[51] Y. Gu, X.L. Shi, L. Pan, W.D. Liu, Q. Sun, X. Tang, L.Z. Kou, Q.F. Liu, Y.F. Wang, Z.G. Chen, Adv. Funct. Mater. 31 (25) (2021) 2101289.

[52] M. Acharya, S.S. Jana, M. Ranjan, T. Maiti, Nano Energy 84 (2021) 105905.

[53] J. Mao, Z. Liu, J. Zhou, H. Zhu, Q. Zhang, G. Chen, Z. Ren, Adv. Phys. 67 (2) (2018) 69-147.

[54] G. Rogl, A. Grytsiv, K. Yubuta, S. Puchegger, E. Bauer, C. Raju, R.C. Mallik, P. Rogl, Acta Mater. 95 (2015) 201-211.

[55] X.L. Huang, D.W. Ao, T.B. Chen, Y.X. Chen, F. Li, S. Chen, G.X. Liang, X.H. Zhang, Z.H. Zheng, P. Fan, Mater. Today Energy 21 (2021) 100743.

[56] H. Liu, X. Shi, F. Xu, L. Zhang, W. Zhang, L. Chen, Q. Li, C. Uher, T. Day, G.J. Snyder, Nat. Mater. 11 (5) (2012) 422-425.

[57] W.-D. Liu, L. Yang, Z.-G. Chen, Nano Today 35 (2020) 100938.

[58] J. Ding, W. Zhao, W. Jin, C.-a. Di, D. Zhu, Adv. Funct. Mater. 31 (20) (2021) 2010695.

[59] N.G. Patel, P.G. Patel, Solid State Electron. 35 (9) (1992) 1269-1272.

[60] S. Jindal, S. Singh, G.S.S. Saini, S.K. Tripathi, Mater. Res. Bull. 145 (2022) 111525.

[61] M. Tan, X.-L. Shi, W.-D. Liu, M. Li, Y. Wang, H. Li, Y. Deng, Z.-G. Chen, Adv. Energy Mater.

11 (40) (2021) 2102578.

[62] M. Tan, W.-D. Liu, X.-L. Shi, J. Shang, H. Li, X. Liu, L. Kou, M. Dargusch, Y. Deng, Z.-G. Chen, Nano Energy 78 (2020) 105379.

[63] M. Tan, W.-D. Liu, X.-L. Shi, H. Gao, H. Li, C. Li, X.-B. Liu, Y. Deng, Z.-G. Chen, Small Methods 3 (11) (2019) 1900582.

[64] D.-W. Ao, W.-D. Liu, Y.-X. Chen, M. Wei, B. Jabar, F. Li, X.-L. Shi, Z.-H. Zheng, G.-X. Liang, X.-H. Zhang, P. Fan, Z.-G. Chen, Adv. Sci. (2021) 2103547.

[65] Y. Wang, M. Hong, W.-D. Liu, X.-L. Shi, S.-D. Xu, Q. Sun, H. Gao, S. Lu, J. Zou, Z.-G. Chen, Chem. Eng. J. 397 (2020) 125360.

[66] L. Liang, H. Lv, X.-L. Shi, Z. Liu, G. Chen, Z.-G. Chen, G. Sun, Mater. Horiz. 8 (1) (2021) 275-276.

[67] H. Shi, C. Liu, Q. Jiang, J. Xu, Adv. Electron. Mater. 1 (4) (2015) 1500017.

[68] L. Zhang, X.-L. Shi, Y.-L. Yang, Z.-G. Chen, Mater. Today 46 (2021) 62-108.

[69] S. Xu, M. Hong, X. Shi, M. Li, Q. Sun, Q. Chen, M. Dargusch, J. Zou, Z.-G. Chen, Energy Environ. Sci. 13 (1) (2020) 348-3488.

[70] Y. Wang, L. Yang, X.-L. Shi, X. Shi, L. Chen, M.S. Dargusch, J. Zou, Z.-G. Chen, Adv. Mater. 31 (29) (2019) 1807916.

[71] S. Xu, M. Hong, X.-L. Shi, Y. Wang, L. Ge, Y. Bai, L. Wang, M. Dargusch, J. Zou, Z.-G. Chen, Chem. Mater. 31 (14) (2019) 5238-5244.

[72] T. Cao, X.-L. Shi, J. Zou, Z.-G. Chen, Microstructures 1 (1) (2021) 2021007.

[73] S.T. Keene, T.P.A. van der Pol, D. Zakhidov, C.H.L. Weijtens, R.A.J. Janssen, A. Salleo, Y. van de Burgt, Adv. Mater. 32 (19) (2020) 2000270.

[74] M. Donoval, M. Micjan, M. Novota, J. Nevrela, S. Kovacova, M. Pavuk, P. Juhasz, M. Jagelka, J. Kovac, J. Jakabovic, M. Cigan, M. Weis, Appl. Surf. Sci. 395 (2017) 86-91.

[75] W. Fan, L. Liang, B. Zhang, C.-Y. Guo, G. Chen, J. Mater. Chem. A 7 (22) (2019) 13687-13694.

[76] K.E. Aasmundtveit, E.J. Samuelsen, O. Inganäs, L.A.A. Pettersson, T. Johansson, S. Ferrer, Synth. Met. 113 (1) (2000) 93-97.

[77] S. Xu, X.-L. Shi, M. Dargusch, C. Di, J. Zou, Z.-G. Chen, Prog. Mater. Sci. 121 (2021) 100840.

[78] I. Imae, R. Akazawa, Y. Ooyama, Y. Harima, J. Polym. Sci. 58 (21) (2020) 3004-3008.

[79] I. Imae, R. Akazawa, Y. Harima, Phys. Chem. Chem. Phys. 20 (2) (2017) 738-741.

[80] C. Yi, A. Wilhite, L. Zhang, R. Hu, S.S.C. Chuang, J. Zheng, X. Gong, ACS Appl. Mater. Interfaces 7 (17) (2015) 8984-8989.

[81] I. Imae, M. Shi, Y. Ooyama, Y. Harima, J. Phys. Chem. C 123 (7) (2019) 4002-4006.

[82] Y. Hu, D. Zhu, Z. Zhu, E. Liu, B. Lu, J. Xu, F. Zhao, J. Hou, H. Liu, F. Jiang, ChemPhysChem 17 (14) (2016) 2256-2262.

[83] W. Deng, L. Deng, Y. Hu, Y. Zhang, G. Chen, Soft Science 1 (3) (2021) 14.

[84] I. Imae, H. Yamane, K. Imato, Y. Ooyama, Compos. Commun. 27 (2021) 100897.

[85] L. Zhang, Y. Harima, I. Imae, Org. Electron. 51 (2017) 304-307.

[86] R. Luo, H. Li, B. Du, S. Zhou, Y. Zhu, Org. Electron. 76 (2020) 105451.

[87] I. Imae, H. Kataoka, Y. Harima, Mol. Cryst. Liq. Cryst 685 (1) (2019) 100-106.

[88] C.T. Hong, Y.H. Kang, J. Ryu, S.Y. Cho, K.-S. Jang, J. Mater. Chem. A 3 (43) (2015) 21428-21433.

[89] H. Li, Y. Liu, P. Li, S. Liu, F. Du, C. He, ACS Appl. Mater. Interfaces 13 (5) (2021) 6650-6658.

[90] C. Xin, Z. Hu, Z. Fang, M. Chaudhary, H. Xiang, X. Xu, L. Aigouy, Z. Chen, Mater. Today Energy

22 (2021) 100859.

[91] M.N. Hasan, H. Wahid, N. Nayan, M.S. Mohamed Ali, Int. J. Energy Res. 44 (8) (2020) 6170-6222.

[92] W.-Y. Chen, X.-L. Shi, J. Zou, Z.-G. Chen, Nano Energy 81 (2021) 105684.

[93] A.I. Boukai, Y. Bunimovich, J. Tahir-Kheli, J.-K. Yu, W.A. Goddard Iii, J.R. Heath, Nature 451 (7175) (2008) 168-171.

[94] V. Schmidt, J.V. Wittemann, S. Senz, U. Gösele, Adv. Mater. 21 (25-26) (2009) 2681-2702.

[95] L. Rauscher, S. Fujimoto, H.T. Kaibe, S. Sano, Meas. Sci. Technol. 16 (5) (2005) 1054-1060.

[96] R.Y. Nuwayhid, F. Moukalled, N. Noueihed, Energy Convers. Manag. 41 (9) (2000) 891-914.

[97] S. Sharma, V.K. Dwivedi, S.N. Pandit, Int. J. Energy Res. 38 (2) (2014) 213-222.

[98] H. Ohta, K. Sugiura, K. Koumoto, Inorg. Chem. 47 (19) (2008) 8429-8436.

[99] G.J. Snyder, A.H. Snyder, Energy Environ. Sci. 10 (11) (2017) 2280-2283.

[100] B. Dörling, J.D. Ryan, J.D. Craddock, A. Sorrentino, A.E. Basaty, A. Gomez, M. Garriga, E. Pereiro, J.E. Anthony, M.C. Weisenberger, A.R. Goñi, C. Müller, M. Campoy-Quiles, Adv. Mater. 28 (14) (2016) 2782-2789.

[101] T. Nguyen Huu, T. Nguyen Van, O. Takahito, Appl. Energy 210 (2018) 467-476.

[102] M. Gu, S. Bai, J. Wu, J. Liao, X. Xia, R. Liu, L. Chen, J. Mater. Res. 34 (7) (2019) 1179-1187.

[103] X. Wang, H. Wang, W. Su, T. Wang, M.A. Madre, J. Zhai, T. Chen, A. Sotelo, C. Wang, J. Mater. Chem. A 8 (6) (2020) 3379-3389.

[104] Y. Zhong, L. Zhang, V. Linseis, B. Qin, W. Chen, L.-D. Zhao, H. Zhu, Nano Energy 72 (2020) 104742.

[105] Y. Wang, Y. Shi, D. Mei, Z. Chen, Appl. Energy 205 (2017) 710-719.

[106] W.-H. Chen, C.-Y. Liao, C.-I. Hung, Appl. Energy 89 (1) (2012) 464-473.

[107] M. Fujii, H. Fujioka, T. Oku, N. Tanaka, H. Imoto, Y. Maruta, S. Nomura, K. Kajiwara, T. Saito, T. Yamakawa, T. Yamakawa, M. Suzuki, Neurol. Med. -Chir. 50 (9) (2010) 839-844.

[108] S.B. Inayat, K.R. Rader, M.M. Hussain, Sci. Rep. 2 (1) (2012) 841.

[109] Y. Eom, D. Wijethunge, H. Park, S.H. Park, W. Kim, Appl. Energy 206 (2017) 649-656.

[110] Z. Fan, J. Ouyang, Adv. Electron. Mater. 5 (11) (2019) 1800769.

[111] G.H. Kim, L. Shao, K. Zhang, K.P. Pipe, Nat. Mater. 12 (8) (2013) 719-723.

[112] S.L. Kim, K. Choi, A. Tazebay, C. Yu, ACS Nano 8 (3) (2014) 2377-2386.

[113] Y. Sun, P. Sheng, C. Di, F. Jiao, W. Xu, D. Qiu, D. Zhu, Adv. Mater. 24 (7) (2012) 932-937.

[114] N. Toshima, K. Oshima, H. Anno, T. Nishinaka, S. Ichikawa, A. Iwata, Y. Shiraishi, Adv. Mater. 27 (13) (2015) 2246-2251.

[115] D. Madan, Z. Wang, P.K. Wright, J.W. Evans, Appl. Energy 156 (2015) 587-592.

[116] Z. Lu, H. Zhang, C. Mao, C.M. Li, Appl. Energy 164 (2016) 57-63.

[117] Z. Lu, M. Layani, X. Zhao, L.P. Tan, T. Sun, S. Fan, Q. Yan, S. Magdassi, H.H. Hng, Small 10 (17) (2014) 3551-3554.

[118] K.K. Jung, Y. Jung, C.J. Choi, J.M. Lee, J.S. Ko, Curr. Appl. Phys. 16 (10) (2016) 1442-1448.

[119] J.H. We, S.J. Kim, B.J. Cho, Energy 73 (2014) 506-512.

[120] M.-K. Kim, M.-S. Kim, S. Lee, C. Kim, Y.-J. Kim, Smart Mater. Struct. 23 (10) (2014) 105002.

[121] S.H. Park, S. Jo, B. Kwon, F. Kim, H.W. Ban, J.E. Lee, D.H. Gu, S.H. Lee, Y. Hwang, J.-S. Kim, D.-B. Hyun, S. Lee, K.J. Choi, W. Jo, J.S. Son, Nat. Commun. 7 (1) (2016) 13403.

[122] D. Madan, Z. Wang, A. Chen, P.K. Wright, J.W. Evans, ACS Appl. Mater. Interfaces 5 (22) (2013) 11872-11876.

[123] S.H. Zaferani, M.W. Sams, R. Ghomashchi, Z.-G. Chen, Nano Energy 90 (2021) 106572.

[124] N.F. Güler, R. Ahiska, Appl. Therm. Eng. 22 (11) (2002) 1271-1276.

[125] Y. Dobrovolsky, Semicond. Phys. Quantum Electron. Optoelectron. 18 (4) (2015) 443-447.

[126] T.A. Ismailov, O.V. Yevdulov, I.S. Mispakhov, A.P. Adamov, Biomed. Eng. 54 (4) (2020) 240-243.

[127] J. Fernandes, P. Anacleto, L.A. Rocha, J. Gaspar, P.M. Mendes, 2017 IEEE 19th Electronics Packaging Technology Conference (EPTC)2017, pp. 1-4.

[128] Y. Duan, X. Wang, Z. Li, J. Ma, IOP Conference Series: Materials Science and Engineering, IOP Publishing2020, pp. 062038.

[129] Z. Slanina, M. Uhlik, V. Sladecek, IFAC-PapersOnLine 51 (6) (2018) 54-59.

[130] Y. Yang, X.-J. Wei, J. Liu, J. Phys. D 40 (18) (2007) 5790-5800.

[131] L.M. Katz, A.S. Young, J.E. Frank, Y. Wang, K. Park, Brain Res. 1017 (1) (2004) 85-91.

[132] G.L. Clifton, S. Allen, J. Berry, S.M. Koch, J. Neurotrauma 9 Suppl 2 (1992) S487-495.

[133] R. Gal, I. Cundrle, I. Zimova, M. Smrcka, Clin. Neurol. Neurosurg. 104 (4) (2002) 318-321.

[134] G. Clifton, J. Neurosurg. 93 (4) (2000) 718-719.

[135] P.S. Midulla, A. Gandsas, A.M. Sadeghi, C.K. Mezrow, M.E. Yerlioglu, W. Wang, D. Wolfe, M.A. Ergin, R.B. Griepp, J. Card. Surg. 9 (5) (1994) 560-575.

[136] D.J. Thurman, E. Beghi, C.E. Begley, A.T. Berg, J.R. Buchhalter, D. Ding, D.C. Hesdorffer, W.A. Hauser, L. Kazis, R. Kobau, B. Kroner, D. Labiner, K. Liow, G. Logroscino, M.T. Medina, C.R. Newton, K. Parko, A. Paschal, P.-M. Preux, J.W. Sander, A. Selassie, W. Theodore, T. Tomson, Wiebe, Epilepsia 52 (s7) (2011) 2-26.

[137] S.L. Moshé, E. Perucca, P. Ryvlin, T. Tomson, Lancet 385 (9971) (2015) 884-898.

[138] M. Baldwin, L.L. Frost, Science 124 (3228) (1956) 931-932.

[139] A.K. Ommaya, M. Baldwin, J. Neurosurg. 20 (1) (1963) 8-20.

[140] X.F. Yang, J.H. Chang, S.M. Rothman, Epilepsia 44 (12) (2003) 1500-1505.

[141] X.-F. Yang, S.M. Rothman, Ann. Neurol. 49 (6) (2001) 721-726.

[142] H.E. Bakken, H. Kawasaki, H. Oya, J.D.W. Greenlee, M.A. Howard, J. Neurosurg. 99 (3) (2003) 604-608.

[143] T. Tokiwa, L. Zimin, H. Ishiguro, T. Inoue, H. Kajigaya, S. Nomura, M. Suzuki, T. Yamakawa, IEEE. Trans. Biomed. Eng. 66 (11) (2019) 3168-3175.

[144] A. Faghri, J. Heat Transfer 134 (12) (2012) 123001.

[145] M.R. Holm, G.A. Poland, Vaccine 39 (3) (2021) 457-459.

[146] A.F. Siqueira, A. Vieira, G.V. Ramos, R.d.C. Marqueti, T.d.F. Salvini, G.O. Puntel, J.L.Q. Durigan, Redox Rep. 22 (6) (2017) 323-329.

[147] C.M. Bleakley, S.M. McDonough, D.C. MacAuley, Br. J. Sports Med. 40 (8) (2006) 700-705.

[148] A. Huang, J.M. McCall, M.D. Weston, P. Mathur, H. Quinn, D.C. Henderson, T.G. Allen-Mersh, Br. J. Surg. 89 (3) (2002) 303-310.

[149] J.W. Castellani, A.J. Young, Auton. Neurosci.: Basic Clin. 196 (2016) 63-74.

[150] Z. Sun, Front. Biosci. (Elite Ed). 2 (2010) 495-503.

[151] A. Golant, R.M. Nord, N. Paksima, M.A. Posner, J. Am. Acad. Orthop. Surg. 16 (12) (2008) 704-715.

[152] D.H. Haynes, W.P. Monaghan, Mil. Med. 149 (4) (1984) 184-188.

[153] Z. Liu, Y. Wang, J. Mao, H. Geng, J. Shuai, Y. Wang, R. He, W. Cai, J. Sui, Z. Ren, Adv. Energy Mater. 6 (7) (2016) 1502269.

[154] Y. Feng, L. Chen, F. Meng, F. Sun, J. Non-Equilib. Thermodyn. 43 (1) (2018) 75-86.

[155] B. Diouf, R. Pode, Renew. Energy 76 (2015) 375-380.

[156] A. Suwardi, S.H. Lim, Y. Zheng, X. Wang, S.W. Chien, X.Y. Tan, Q. Zhu, L.M.N. Wong, J. Cao, W. Wang, Q. Yan, C.K.I. Tan, J. Xu, J. Mater. Chem. C 8 (47) (2020) 16940-16948.

[157] A. Suwardi, F. Wang, K. Xue, M.-Y. Han, P. Teo, P. Wang, S. Wang, Y. Liu, E. Ye, Z. Li, X.J. Loh, Adv. Mater. 34 (1) (2022) 2102703.

[158] Z. Wang, V. Leonov, P. Fiorini, C. Van Hoof, Sens. Actuator A Phys. 156 (1) (2009) 95-102.

[159] M. Thielen, L. Sigrist, M. Magno, C. Hierold, L. Benini, Energy Convers. Manag. 131 (2017) 44-54.

[160] N.H. Cox, P. Dyson, Br. J. Dermatol. 133 (1) (1995) 60-65.

[161] C. Gayner, K.K. Kar, W. Kim, Mater. Today Energy 9 (2018) 359-376.

[162] C. Gayner, Y. Amouyal, Adv. Funct. Mater. 30 (18) (2020) 1901789.

[163] J.R. Sootsman, D.Y. Chung, M.G. Kanatzidis, Angew. Chem. Int. Ed. 48 (46) (2009) 8616-8639.

[164] C. Gayner, K.K. Kar, Prog. Mater. Sci. 83 (2016) 330-382.

[165] Y. Thimont, S. LeBlanc, J. Appl. Phys. 126 (9) (2019) 095101.

[166] J. Yan, X. Liao, D. Yan, Y. Chen, J. Microelectromechanical Syst. 27 (1) (2018) 1-18.

[167] W.-Y. Chen, X.-L. Shi, J. Zou, Z.-G. Chen, Small Methods (2022) 2101235.

[168] Y. Cai, W.-W. Wang, C.-W. Liu, W.-T. Ding, D. Liu, F.-Y. Zhao, Renew. Energy 147 (2020) 1565-1583.

[169] H. Luo, Y. Zhu, Z. Xu, Y. Hong, P. Ghosh, S. Kaur, M. Wu, C. Yang, M. Qiu, Q. Li, Nano Lett. 21 (9) (2021) 3879-3886.

[170] Y. Zheng, C. Liu, L. Miao, C. Li, R. Huang, J. Gao, X. Wang, J. Chen, Y. Zhou, E. Nishibori,

Nano Energy 59 (2019) 311-320.

[171] X.-L. Shi, X. Tao, J. Zou, Z.-G. Chen, Adv. Sci. 7 (7) (2020) 1902923.

[172] F. Kim, B. Kwon, Y. Eom, J.E. Lee, S. Park, S. Jo, S.H. Park, B.-S. Kim, H.J. Im, M.H. Lee, T.S. Min, K.T. Kim, H.G. Chae, W.P. King, J.S. Son, Nat. Energy 3 (4) (2018) 301-309.

[173] Q. Shi, J. Sun, C. Hou, Y. Li, Q. Zhang, H. Wang, Adv. Fiber Mater. 1 (1) (2019) 3-31.

[174] X. Zhang, T.-T. Li, H.-T. Ren, H.-K. Peng, B.-C. Shiu, Y. Wang, C.-W. Lou, J.-H. Lin, ACS Appl. Mater. Interfaces 12 (49) (2020) 55072-55082.